AMERICAN SOCIETY FOR MICROBIOLOGY | mBio®

RESEARCH ARTICLE

Staphylococcus aureus Uses the GraXRS Regulatory System To Sense and Adapt to the Acidified Phagolysosome in Macrophages

Ronald S. Flannagan,[a] Robert C. Kuiack,[a] Martin J. McGavin,[a] David E. Heinrichs[a]

[a]Department of Microbiology and Immunology, the University of Western Ontario, London, Ontario, Canada

ABSTRACT Macrophages are critical to innate immunity due to their ability to phagocytose bacteria. The macrophage phagolysosome is a highly acidic organelle with potent antimicrobial properties, yet remarkably, ingested *Staphylococcus aureus* replicates within this niche. Herein we demonstrate that *S. aureus* requires the GraXRS regulatory system for growth within this niche, while the SaeRS and AgrAC two-component regulatory systems and the α-phenol soluble modulins are dispensable. Importantly, we find that it is exposure to acidic pH that is required for optimal growth of *S. aureus* inside fully acidified macrophage phagolysosomes. Exposure of *S. aureus* to acidic pH evokes GraS signaling, which in turn elicits an adaptive response that endows the bacteria with increased resistance to antimicrobial effectors, such as antimicrobial peptides, encountered inside macrophage phagolysosomes. Notably, pH-dependent induction of antimicrobial peptide resistance in *S. aureus* requires the GraS sensor kinase. GraS and MprF, a member of the GraS regulon, play an important role for bacterial survival in the acute stages of systemic infection, where in murine models of infection, *S. aureus* resides within liver-resident Kupffer cells. We conclude that GraXRS represents a vital regulatory system that functions to allow *S. aureus* to evade killing, prior to commencement of replication, within host antibacterial immune cells.

IMPORTANCE *S. aureus* can infect any site of the body, including the microbicidal phagolysosome of the macrophage. The ability of *S. aureus* to infect diverse niches necessitates that the bacteria be highly adaptable. Here we show that *S. aureus* responds to phagolysosome acidification to evoke changes in gene expression that enable the bacteria to resist phagolysosomal killing and to promote replication. Toxin production is dispensable for this response; however, the bacteria require the sensor kinase GraS, which transduces signals in response to acidic pH. GraS is necessary for phagolysosomal replication and survival of *S. aureus* in the acute stage of systemic infection. Disruption of this *S. aureus* adaptation would render *S. aureus* susceptible to phagocyte restriction.

KEYWORDS antimicrobial peptides, host-pathogen, intracellular bacteria, macrophages, phagocytosis, phagolysosome

Staphylococcus aureus is a notorious bacterial human and animal pathogen that is recognized as a serious threat to health care. Although *S. aureus* was once considered a nosocomial pathogen, it is evident that methicillin-resistant *S. aureus* (MRSA) strains, such as USA300 LAC, display enhanced virulence and can be disseminated throughout the community at large (1–3). Incredibly, *S. aureus* can colonize virtually every tissue of the body (4–7), and this propensity to cause infection can, in part, be attributed to the exceptional ability of *S. aureus* to circumvent host immunity. This is largely due to the vast repertoire of virulence determinants that *S. aureus* can express.

Received 23 May 2018 **Accepted** 18 June 2018 **Published** 17 July 2018

Citation Flannagan RS, Kuiack RC, McGavin MJ, Heinrichs DE. 2018. *Staphylococcus aureus* uses the GraXRS regulatory system to sense and adapt to the acidified phagolysosome in macrophages. mBio 9:e01143-18. https://doi.org/10.1128/mBio.01143-18.

Editor Victor J. Torres, New York University School of Medicine

Address correspondence to David E. Heinrichs, deh@uwo.ca.

A subset of these virulence factors are toxins (e.g., leucocidins) that poison host immune cells, such as macrophages and neutrophils, from the extracellular milieu, driven by the expression of host receptors (e.g., CD11b and CCR5) that are displayed at the plasmalemma of affected cells (reviewed in references 8 and 9). Despite this, neutrophils and macrophages are critical for host defense against *S. aureus* infection.

Professional phagocytes such as macrophages are central to innate immunity due to their ability to phagocytose particulates, including bacteria (10). Ingested microbes are internalized into membrane-bound vacuoles termed phagosomes that undergo maturation and become highly microbicidal organelles termed phagolysosomes (11). A hallmark of phagolysosome formation is the marked acidification of the phagosome lumen to a pH of ~5.4 or less due to the activity of the vacuolar ATPase (V-ATPase) proton pump (12, 13). Despite the antimicrobial activity of the phagolysosome, macrophages fail to eradicate internalized *S. aureus* cells (14–17). After phagocytosis of *S. aureus* USA300 by macrophages, the bacteria reside within mature lysosome-associated membrane protein-1 (LAMP-1)-positive phagolysosomes, where bacterial replication commences (15, 16). Interestingly growth of *S. aureus* within the macrophage is significantly delayed (15, 16). How *S. aureus* overcomes the antimicrobial aspects of the phagolysosome and grows in this niche is unknown. In the present study, we demonstrate that toxin production is dispensable for growth in the *S. aureus*-containing phagosome (SaCP). In contrast, we find phagolysosomal growth of *S. aureus* requires the GraXRS regulatory system. Moreover, through GraS, *S. aureus* can perceive phagolysosome acidification and elicit adaptive responses that engender phagolysosomal bacteria with the ability to resist killing and replicate. Finally, a murine model of systemic infection reveals that GraS is required for optimal survival in the acute stages of systemic infections when the bacteria reside within liver-resident Kupffer cells.

RESULTS

***S. aureus* growth in macrophages occurs independently of toxin production.** In the extracellular environment, *S. aureus* elaborates toxins that poison immune cells such as macrophages. However, whether toxin production is important for the onset of *S. aureus* replication within the macrophage is unclear. Previous work has suggested that *S. aureus* may require either the Agr quorum sensing system or expression of alpha-toxin or alpha phenol soluble modulins (PSMα peptides) to survive and replicate within macrophages (18–20). Incongruent with these reports, it has been shown, both *in vitro* and *in vivo*, that *S. aureus* commences replication within macrophages while confined to acidic, LAMP-1-positive phagolysosomes (15, 16). Therefore, to further investigate the role of these genes and toxin production in the onset of *S. aureus* growth in the phagolysosome of macrophages, we constructed mutant strains of *S. aureus* USA300 lacking the entire *agrBDCA* locus (*agr*) and the *psm*α_{1-4} genes (*psm*α), a strain carrying a transposon-interrupted *saeR* gene (*saeR*::φNΣ), and a strain carrying all three mutations (*agr psm*α *sae*) (see Table 1 for descriptions). The *agr* and *sae* loci are global regulators of *S. aureus* virulence and are required for toxin production in *S. aureus* (21, 22). As expected, USA300 strains deficient for SaeR and/or Agr signaling demonstrated a lack of hemolytic activity on blood agar plates compared to wild-type (WT) *S. aureus* USA300 (see Fig. S1A in the supplemental material), consistent with previous reports (23, 24). Moreover, in contrast to wild-type bacteria, *S. aureus* strains deficient for *agr*, *psm*α, and *sae* also fail to intoxicate primary human macrophage colony-stimulating factor (M-CSF)-derived macrophages from the extracellular milieu, indicating a defect in toxin production (Fig. S1B). To assess whether these strains were indeed defective for growth within macrophages, gentamicin protection assays were performed using RAW 264.7 (here referred to as RAW) cells infected with wild-type *S. aureus* USA300 and each of the aforementioned mutants. This analysis revealed that at 12 h postinfection (hpi), each strain demonstrated at least a 9-fold increase in CFU per milliliter over that recovered for the same strain at 1.5 hpi (Fig. 1A). Moreover, there was no significant difference between wild-type *S. aureus* or the mutants in their ability to replicate within RAW macrophages (Fig. 1A). This was also evident when replication

TABLE 1 Bacterial strains and plasmids used in this study

Bacterial strain or plasmid	Description[a]	Source or reference
Strains		
S. aureus		
USA300	USA300 LAC; hypervirulent community-associated MRSA; cured of antibiotic resistance plasmid	Laboratory stock
Newman	Wild-type clinical osteomyelitis isolate	55
RN4220	r_K^- m_K^+; capable of accepting foreign DNA	56
saeR mutant	Derivative of *S. aureus* USA300 with *saeR*::φNΣ transduced from the Nebraska transposon library; Ery^r	This study
agr psmα mutant	Derivative of *S. aureus* USA300 with Δ*psmα*$_{1-4}$ and *agr*::*tetM*; Tet^r	This study
saeR agr psmα mutant	Derivative of *S. aureus* USA300 with Δ*psmα*$_{1-4}$ and *agr*::*tetM* and with *saeR*::φNΣ transduced from the Nebraska transposon mutant library; Tet^r Ery^r	This study
graS mutant	Derivative of *S. aureus* USA300 with Δ*graS* created by pKOR mutagenesis	This study
mprF mutant	Derivative of *S. aureus* USA300 JE2 from the Nebraska transposon library carrying *mprF*::φNΣ; Ery^r	This study
Newman *graS*	*S. aureus* strain Newman with *graS*::φNΣ allele transduced from the Nebraska transposon library; Ery^r	This study
E. coli DH5α	F$^-$ ϕ80d*lacZ*ΔM15 *recA1 endA1 gyrA96 thi-1 hsdR17*(r_K^- m_K^+) *supE44 relA1 deoR* Δ(*lacZYA-argF*)*U169 phoA* λ$^-$	Laboratory stock
Plasmids		
pAH9	Constitutive staphylococcal mCherry expression vector; Ery^r	57
P_{prsA}::*gfp*	Constitutive *S. aureus* GFP expression vector; Amp^r Ery^r	58
pCG44	*E. coli*/*S. aureus* shuttle vector for constitutive expression of pHluorin in *S. aureus*; Amp^r Cm^r	59
pKOR	*E. coli*/*S. aureus* shuttle vector for creation of unmarked gene deletions in staphylococcal spp.; Amp^r Cm^r	51
pKOR-GraS	pKOR with regions of homology to delete *graS*	This study
pKOR-αPSM	pKOR with regions of homology to delete *psmα*$_{1-4}$	This study
pALC2073	*E. coli*/*S. aureus* shuttle vector; Amp^r Cm^r	60
pGraS	pALC2073 with *graS* from *S. aureus* USA300	This study
pGYLux	Promoterless bioluminescent reporter plasmid encoding *luxABCDE*; Amp^r Cm^r	61
pGYLux::*mprF*	pGYLux with the *mprF* promoter cloned	This study

[a]Ery^r, Tet^r, Amp^r, and Cm^r indicate resistance to erythromycin, tetracycline, ampicillin, and chloramphenicol, respectively.

was investigated at the subcellular level by fluorescence microscopy. Here each strain expressing green fluorescent protein (GFP) was analyzed by fluorescence proliferation assays (see Materials and Methods for details) in conjunction with LAMP-1 immunofluorescence. In brief, just prior to infection, all GFP-expressing bacteria are colabeled with a far-red fluorescent proliferation dye, eFluor-670. As bacteria replicate, the dye is diluted until such time as the dye is no longer detectable on bacterial cells (i.e., replicating bacteria appear GFP positive yet proliferation dye negative). In contrast, bacteria that are unable to proliferate retain the proliferation dye and can thus be easily identified by fluorescence microscopy. This analysis revealed that at 1.5 hpi, none of the strains (i.e., USA300 or any of the mutants) had replicated, as all phagocytosed bacteria remained GFP and eFluor-670 positive (Fig. 1B). In contrast, by 12 hpi, replicating (i.e., GFP-positive, eFluor-670-negative) bacteria were observed within RAW macrophages for each strain (Fig. 1B; see Fig. S2 in the supplemental material). Moreover, immunodetection of LAMP-1 confirmed that wild-type and mutant bacteria are replicating within LAMP-1-positive phagosomes (Fig. 1B; Fig. S2). Importantly, there was no obvious difference in proliferation or LAMP-1 distribution around the *S. aureus*-containing phagosome (SaCP) for each strain. These observations in RAW cells were recapitulated in primary human M-CSF-derived macrophages; both WT and *agr sae psmα* bacteria produced a similar ~6-fold increase in bacterial burden within the 1.5- to 12-h time frame and appeared GFP positive yet eFluor negative when visualized within human M-CSF-derived macrophages (Fig. 1C and D). Taken together, these data reveal that *S. aureus* USA300 does not require *agr*, *sae*, *psmα*, or, by extension, toxin production to commence replication within LAMP-1-positive phagosomes in macrophages.

Replicating *S. aureus* bacteria reside within fully acidified phagolysosomes. Since replication of *S. aureus* in macrophages occurs after a significant delay (~10 to

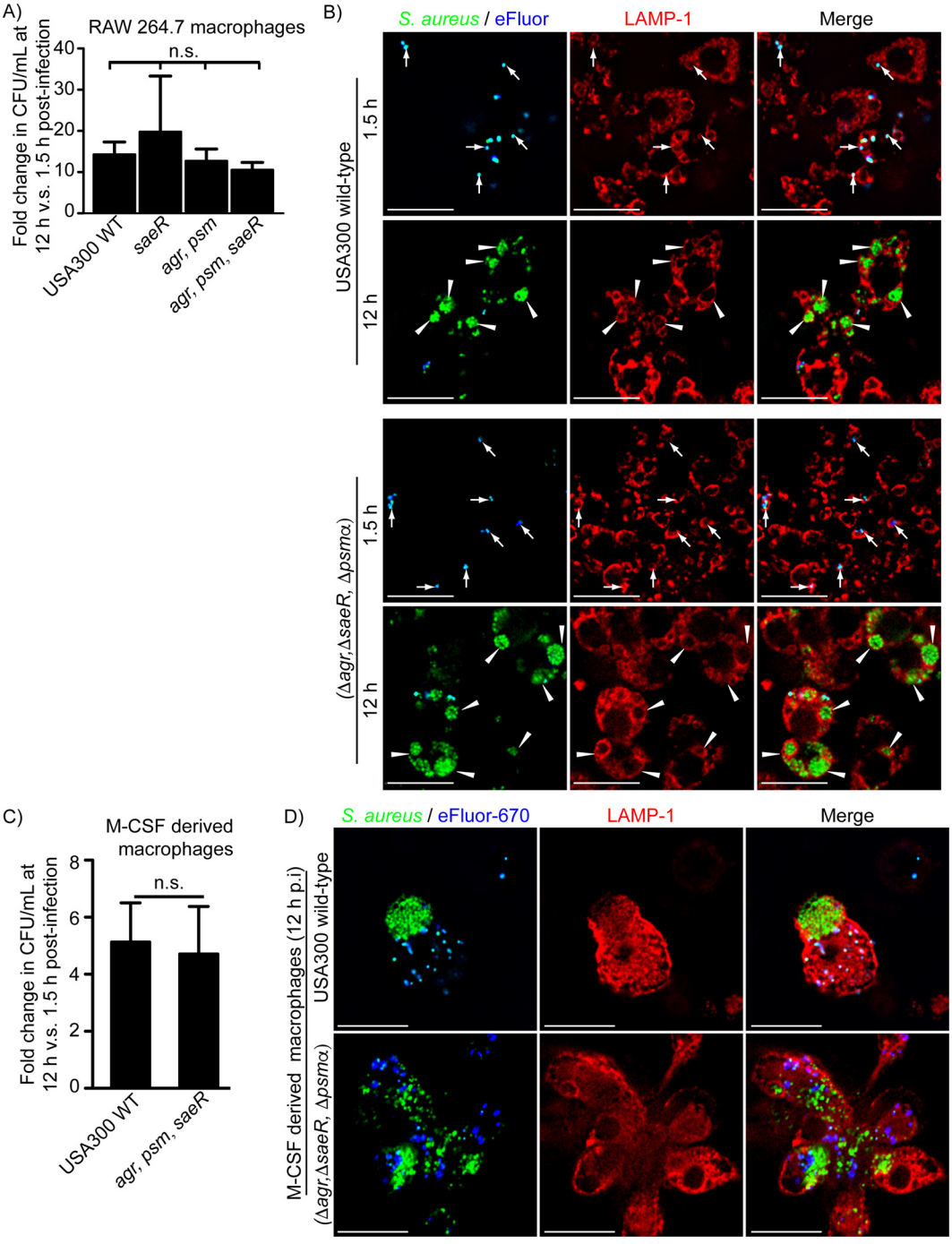

FIG 1 The two-component regulatory systems SaeRS and AgrAC and the PSMα peptides are dispensable for *S. aureus* growth in macrophages. In panel A, the graph depicts the fold change in CFU per milliliter at 12 h versus 1.5 h postinfection for wild-type *S. aureus* USA300 and mutant strains lacking a functional SaeR (*saeR*), Agr (*agr*), and the PSMα peptides (*psm*). The data are the mean ± standard error of the mean (SEM) from at least four independent experiments. n.s. indicates that differences in the data are not statistically significant ($P \geq 0.05$) by one-way ANOVA with a Dunnett's *post hoc* comparison. In panel B, representative images of fluorescence-based proliferation assays using RAW 264.7 macrophages and GFP-expressing wild-type *S. aureus* USA300 (top panels) and the triple mutant lacking the *sae*R, *agr*, and *psm*α genes (bottom panels) are shown. Endogenous LAMP-1 protein (in red) was detected by immunostaining macrophages at 1.5 and 12 h postinfection. GFP-expressing bacteria are green, and at the outset of the infection, all bacteria were labeled with eFluor-670 proliferation dye (in blue). At 12 h postinfection, replicating bacteria appear GFP positive yet far-red negative. The white arrows point to GFP- and eFluor-positive bacteria (i.e., cells that have not replicated). White arrowheads point to GFP-only bacteria that are demarcated by LAMP-1 and therefore growing inside late phagosomes/phagolysosomes inside RAW macrophages at 12 h postinfection. Bars equal ~10 μm. In panel C, the growth of *S. aureus* USA300 and the triple mutant inside primary human M-CSF-derived macrophages is summarized. The data are the mean ± SEM fold change in CFU per milliliter at 12 h versus 1.5 h postinfection for *S. aureus* USA300 and the triple mutant lacking *saeR*, *agr*, and the *psm*α genes. These data derive from 8

(Continued on next page)

12 h) (15, 16), we next sought to establish whether, when replicating intracellularly, *S. aureus* resides within acidified vacuoles, or whether the bacteria have modified the pH of the SaCP. To this end, fluorescent proliferation assays were performed on RAW macrophages infected with mCherry-expressing *S. aureus* cells and also stained with the acidotropic dye LysoTracker Green. Live-cell imaging revealed that at 12 h postinfection, well-defined vacuoles containing replicating *S. aureus* cells accumulate LysoTracker probe. In contrast, pretreatment of RAW macrophages with the V-ATPase inhibitor concanamycin A (ConA) renders infected macrophages completely refractory to LysoTracker staining, indicating that acidification of the SaCP is due to V-ATPase function (Fig. 2A). Moreover, these observations demonstrate that *S. aureus* can commence replicating within intact vacuoles that are acidic within murine macrophages.

To establish that replicating *S. aureus* is indeed inside mature phagolysosomes, we next performed pulse-chase experiments with fluorescein isothiocyanate (FITC)-dextran (25). Macrophages loaded with lysosomal dextran were infected with live or dead *S. aureus* cells, and at ~12 h postinfection macrophages were imaged by live-cell fluorescence microscopy. Previously we demonstrated that 30 min after engulfment, *S. aureus* colocalized with lysosomal dextran (15); however, here we show that even at 12 h postinfection, live and dead bacteria can remain colocalized with FITC-dextran in both RAW and primary human macrophages (Fig. 2B; see Fig. S3 in the supplemental material). Next, we performed quantitative measurement of phagolysosomal pH at 12 h postinfection by performing ratiometric pH measurements using FITC-dextran that is colocalized with intracellular *S. aureus*. These measurements revealed that the luminal pH of the SaCP harboring replicating and nonreplicating bacteria is on average 5.43 $\pm$ 0.16, which is comparable to the measured pH (5.36 $\pm$ 0.13) of phagolysosomes containing dead bacteria (Fig. 2C). The utility of our FITC-dextran to measure dynamic pH changes is evident from clamped dextran-loaded macrophages, where the fluorescence ratio of FITC, when excited at 490 and 430 nm, increases as cells are made more alkaline (Fig. 2C, inset). These data show that phagocytosed *S. aureus* cells can reside within intact phagolysosomes that are acidic, and this is where bacterial replication can commence.

The GraXRS regulatory system is required for growth within macrophage phagolysosomes. In both the *in vitro* and *in vivo* settings, the growth of *S. aureus* in macrophage phagolysosomes is delayed, occurring more than 8 h postinfection (15, 16). Implicit in this observation is that *S. aureus* undergoes adaptation to the phagolysosomal environment, yet how this is accomplished is unknown. There is evidence to suggest that under certain conditions, the survival of *S. aureus* at acidic pH requires the GraXRS regulatory system (26). A hallmark of mature phagolysosomes is their marked acidity and, therefore, we hypothesized that *S. aureus*, as opposed to perforating the SaCP with toxins as we have just described does not occur, may simply adapt to this acidic environment through sensing by the GraXRS regulatory system. A mutant of *S. aureus* USA300 lacking the sensor kinase GraS gene (*graS*) was created, and its ability to survive and proliferate within RAW macrophages was assessed. Analysis of the fold change in CFU per milliliter at 12 h postinfection compared to 1.5 h postinfection revealed that wild-type bacteria increased on average 12.5 $\pm$ 3.9-fold (Fig. 3A). In contrast, the *graS* strain yielded a fold change in CFU per milliliter of 0.95 $\pm$ 0.29-fold during the same time frame, indicating the bacteria failed to grow (Fig. 3A). To visualize the *graS* mutant and confirm the inability of this strain to replicate within RAW macrophages, we also performed fluorescence-based proliferation assays. RAW macrophages were infected with wild-type USA300 or *graS* bacteria expressing GFP that

FIG 1 Legend (Continued)
biological replicate infections using macrophages derived from four independent donors. n.s. indicates the difference between the means is not statistically significant by the Student's unpaired *t* test ($P \geq 0.05$). In panel D, representative micrographs depict wild-type *S. aureus* USA300 (top panels) and the triple mutant lacking *saeR*, *agr*, and the *psm*α genes (bottom) growing inside primary human M-CSF-derived macrophages at 12 h postinfection. Endogenous immunostained LAMP-1 protein is shown in red. Growing bacteria appear as GFP positive (green) yet proliferation dye (in blue) negative. Scale bars equal 10 μm.

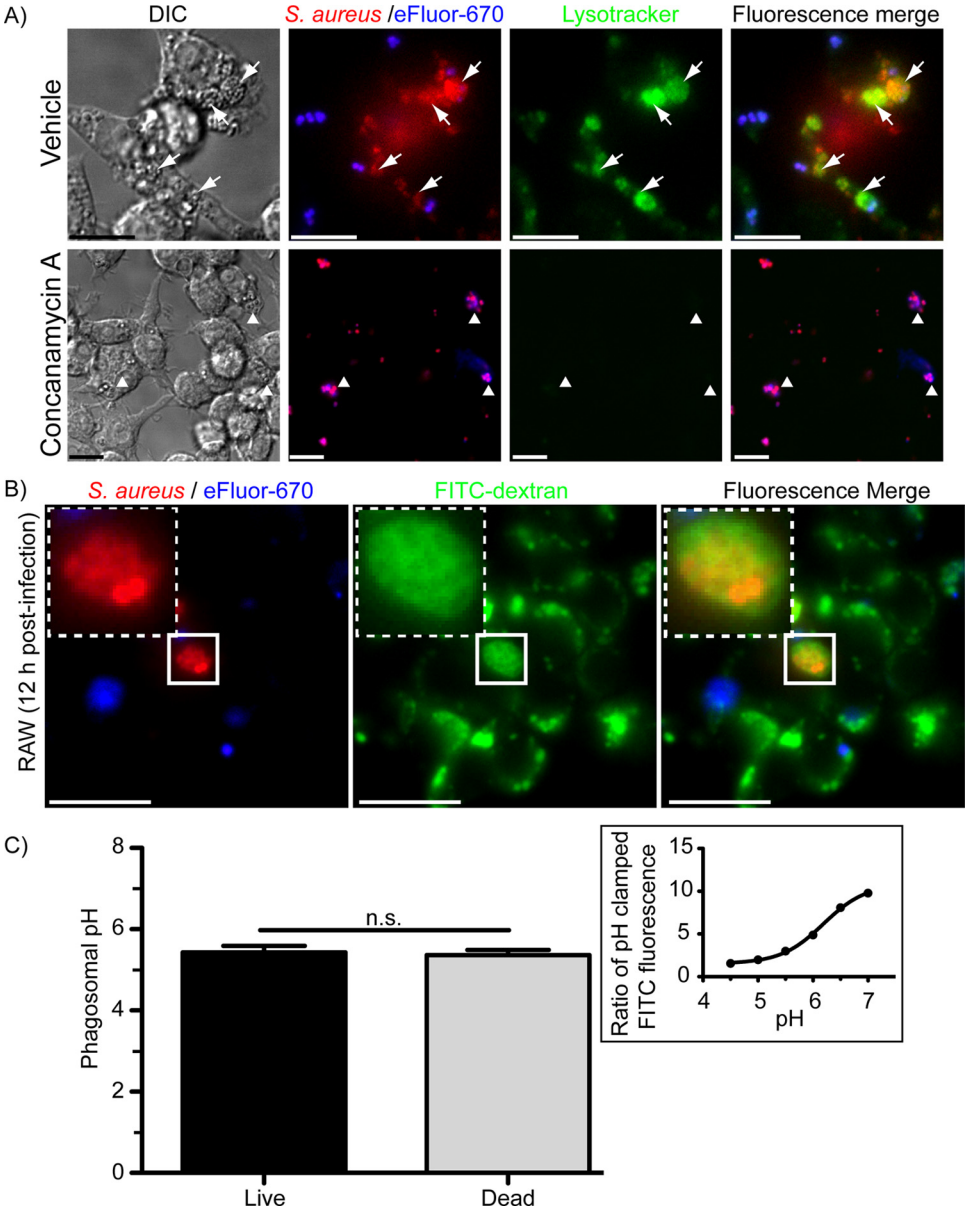

FIG 2 *S. aureus* USA300 replicates inside acidic phagolysosomes. In panel A, the acidity and integrity of the phagolysosomal membrane containing *S. aureus* were assessed by LysoTracker Green DND-26 staining. Macrophages were infected with live *S. aureus* USA300 cells expressing mCherry and labeled with eFluor proliferation dye. At 11 h postinfection, macrophages were left untreated or were treated with 1 μM ConA, and at 12 h postinfection, macrophages were stained with the acidotropic probe LysoTracker and imaged live. In the top panels, the white arrows point to replicating (i.e., eFluor-negative) bacteria that colocalize with LysoTracker Green fluorescence signal. In the bottom panel, the white arrowheads point to bacteria that are intracellular but now in the presence of ConA no longer colocalize with the acidotropic probe. Note not just phagosomes but also endosomes and lysosomes are also refractory to LysoTracker staining. These images are representative of at least three independent experiments. DIC, differential inference contrast. Bars equal ~10 μm. The residence of replicating *S. aureus* inside mature phagolysosomes (B) and pH of the compartment (C) in which these bacteria reside were established by dextran pulse-chase experiments. In panel B, a RAW macrophage loaded with 10,000-MW FITC-dextran and containing live replicating *S. aureus* USA300 at 12 h postinfection is shown. The white box delineates the region of the cell containing a large FITC-dextran-positive phagosome that also contains mCherry-positive yet eFluor-negative *S. aureus* USA300. In panel C, ratiometric pH measurements were made of FITC-dextran fluorescence (excitation 434 nm/excitation 490 nm) to quantify the pH of RAW cell phagolysosomes containing live and dead *S. aureus* USA300 cells. The graph shows the average pH ± standard deviation (SD) for live and dead *S. aureus* USA300 cells at 12 h postinfection. These data are the result of three independent experiments. n.s. indicates not significant as determined by Student's *t* test. The representative graph shown in the inset reveals the pH responsiveness of FITC fluorescence as determined by pH clamping of live macrophages in K^+-rich buffers with 10 μM nigericin.

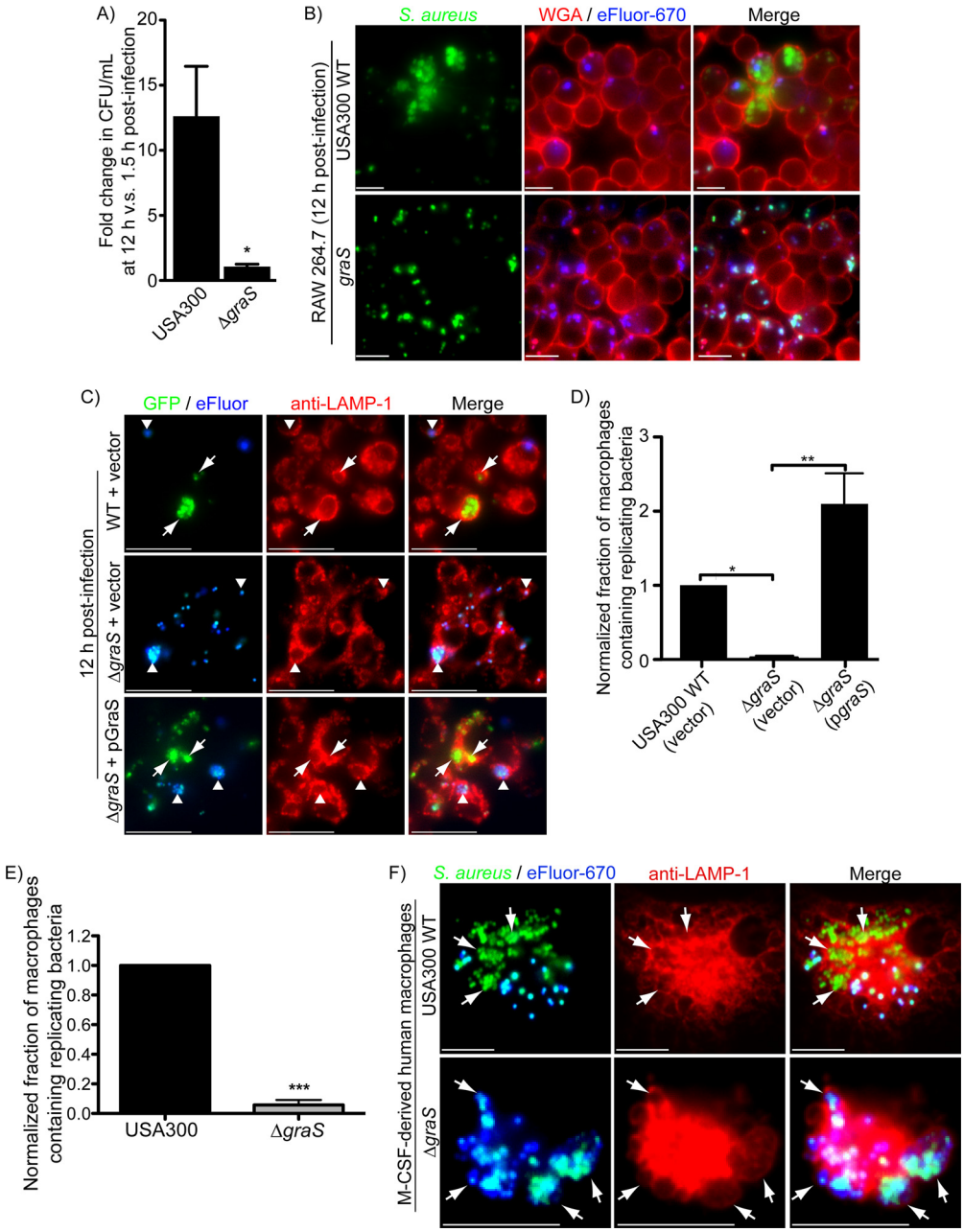

FIG 3 The sensor kinase GraS of the GraXRS regulatory system is required for *S. aureus* proliferation inside macrophages. The ability of *S. aureus* USA300 lacking the *graS* gene to grow inside RAW macrophages was compared to that of wild-type *S. aureus* USA300. In panel A, the fold change in CFU per milliliter at 12 h versus 1.5 h postinfection for wild-type USA300 and *graS* bacteria is shown. The data are the mean ± SEM derived from four independent experiments, and the asterisk indicates $P \leq 0.05$. In panel B, the images depict the intracellular replication of wild-type *S. aureus* and the lack of replication for the *graS* mutant. Bacterial replication was determined by fluorescence proliferation assay, where replicating bacteria at 12 h postinfection are GFP positive and devoid of the proliferation dye. Extracellular bacteria and the macrophage plasmalemma are marked with tetramethyl rhodamine isothiocyanate (TRITC)-conjugated wheat germ agglutinin. These images are representative of several independent infections. In panel C, the fluorescent micrographs depict GFP-expressing bacteria that were employed in fluorescence-based proliferation assays. Shown is wild-type *S. aureus* USA300 carrying empty pALC2073 and the Δ*graS*(pALC2073) and Δ*graS*(pGraS) strains. Replicating bacteria are detected as green yet proliferation dye-negative bacteria at 12 h postinfection. White arrows point to proliferating bacteria, whereas arrowheads point to bacteria that have not replicated and are GFP and proliferation dye positive. Endogenous LAMP-1 protein detected by immunostaining at 12 h postinfection is shown in red. Bars equal 10 μm. These images are representative of three independent experiments. In panel D, the fraction of macrophages containing replicating bacteria normalized to the wild-type USA300 infection is shown. These data are the mean ± SEM from three independent experiments. Significance was determined by one-way ANOVA with Bonferroni's posttest. *, $P < 0.05$; **, $P < 0.001$. In panel E, quantitation of the fraction of primary human M-CSF-derived macrophages containing replicating *graS* mutant bacteria normalized to the wild type is shown. The data are the mean

(Continued on next page)

were colabeled with the far-red proliferation dye, and after gentamicin treatment, infected macrophages were visualized at 1.5 and 12 h postinfection. At the early time point, neither strain had commenced replicating intracellularly (data not shown); however, at 12 h postinfection, macrophages harboring wild-type bacteria contained GFP-positive foci that were eFluor and wheat germ agglutinin (WGA) negative, indicating intracellularly replicating *S. aureus* cells were present (Fig. 3B, top panels). In contrast, the overwhelming majority of phagocytosed *graS* bacteria remained GFP and eFluor positive, indicating this strain has a replication-defective phenotype in macrophages (Fig. 3B, bottom panels), despite there being no detectable difference in their infectivities (see Fig. S4A in the supplemental material). Complementation experiments were performed to confirm the importance of *graS* for intracellular growth. In these experiments, *graS* bacteria carrying a vector control failed to grow within macrophages by 12 h postinfection, whereas wild-type and *graS* bacteria with *graS* expressed from a plasmid grew within RAW macrophages (Fig. 3C and D). Moreover, analysis of LAMP-1 protein confirmed again that wild-type and complemented bacteria replicate within LAMP-1-positive vacuoles (Fig. 3C). Similarly, the *graS* mutant is constrained by LAMP-1-positive membranes; however, these bacteria remain proliferation dye positive (Fig. 3C). Importantly, these data were recapitulated using primary human M-CSF-derived macrophages, where, once again, fluorescence proliferation assays confirmed that *graS*-deficient bacteria fail to replicate by 12 h postinfection (Fig. 3E and F). In summary, these data reveal that *S. aureus* does not alter the pH of the SaCP, instead requiring the sensor kinase GraS to adapt to this compartment prior to the initiation of bacterial replication.

Phagolysosome acidification is a requirement for intracellular growth of *S. aureus*. Given our assertion that *S. aureus* must first sense acidic pH to be able to adapt to the phagolysosome prior to the commencement of replication, it would be reasonable to posit that alkalinization of the phagolysosome would accelerate growth of wild-type *S. aureus*. To test this, we performed fluorescence-based proliferation assays in which phagocytes were treated with ConA or the weak base NH_4Cl after the bacterial trafficking to the phagolysosome (i.e., at 1.5 h postinfection). This analysis revealed that at 12 h postinfection, *S. aureus* had replicated intracellularly; however, inhibitor treatment did not enhance growth compared to that of control macrophages (Fig. 4A). Using the acidotropic dye LysoTracker Red, we could verify that our ConA and NH_4Cl treatment regimen had the intended affect and alkalinized lysosomes as expected (Fig. 4B). In parallel, we performed gentamicin protection assays, which also revealed that ConA or NH_4Cl treatment did not accelerate intracellular growth of *S. aureus* compared to control RAW macrophages (Fig. 4C). Finally, these results were recapitulated in primary human M-CSF-derived macrophages, where fluorescence proliferation assays revealed that ConA and NH_4Cl treatment did not augment *S. aureus* growth (Fig. 4D).

While alkalinization of phagolysosomes alone did not improve bacterial replication, we next considered whether V-ATPase inhibition could protect *graS* bacteria and improve their growth in macrophages. To this end, we infected RAW macrophages with wild-type *S. aureus* USA300 carrying pALC2073 (empty vector), the *S. aureus graS* strain carrying pALC2073, and the *S. aureus graS* strain carrying the complementation plasmid pGraS, and performed gentamicin protection assays to assess changes in bacterial burden inside macrophages over time. To protect *graS* bacteria from any exposure to acid stress, we now pretreated macrophages with ConA, which was maintained

FIG 3 Legend (Continued)
± SEM from three independent experiments in which macrophages were derived from three independent blood donors. Replicating bacteria appeared GFP positive but were negative for the far-red proliferation dye eFluor-670 at 12 h postinfection. Statistical significance was determined by an unpaired *t* test, and the asterisks indicate a *P* value of <0.0001. In panel F, eFluor-labeled GFP-expressing wild-type *S. aureus* USA300 and the *graS* strain are shown in primary human M-CSF-derived macrophages that were immunostained with anti-LAMP-1 antibody at 12 h postinfection. White arrows point to LAMP-1-positive bacteria. Bars equal ~10 μm.

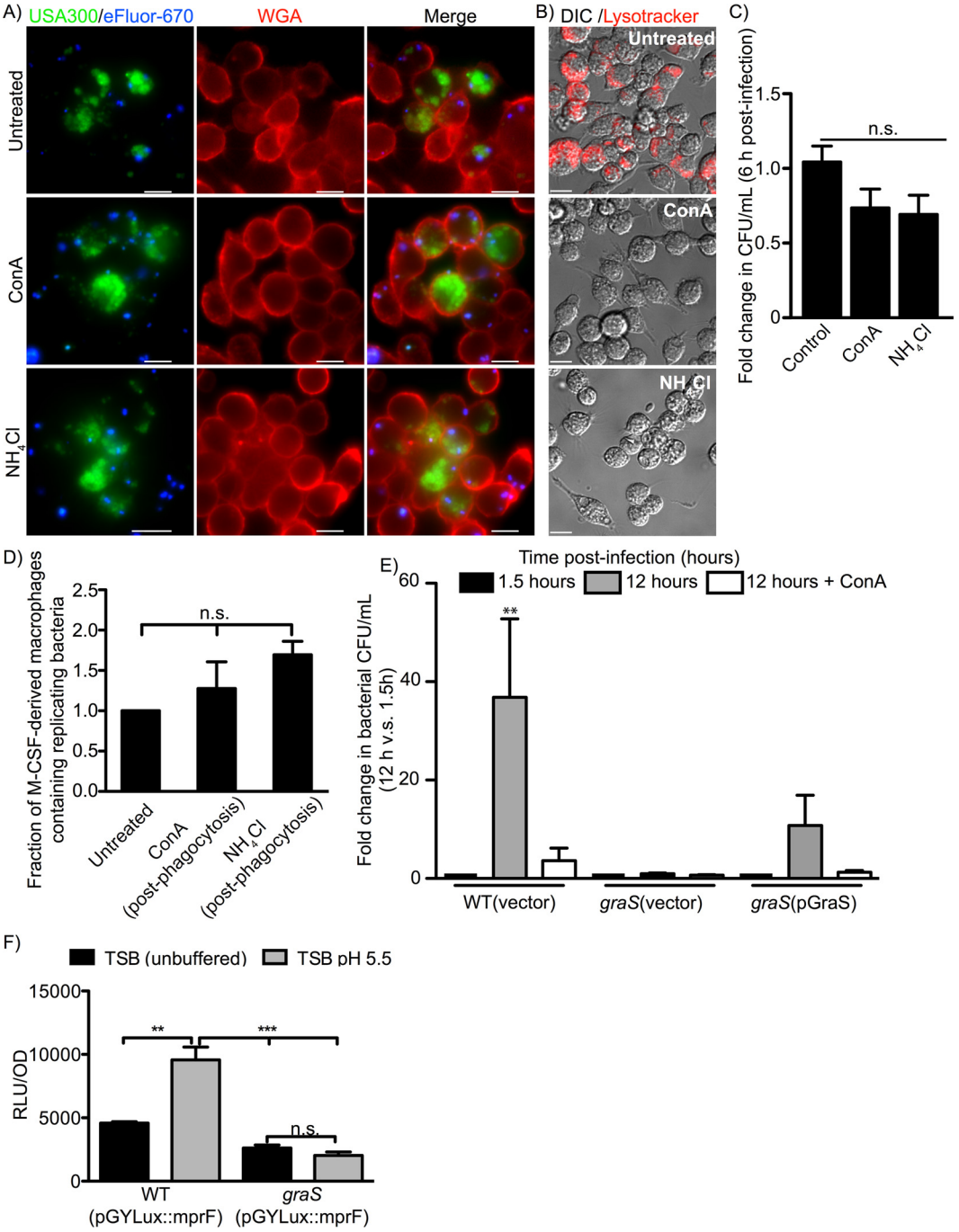

FIG 4 V-ATPase inhibition prior phagocytosis impairs *S. aureus* growth in macrophages, yet alkalinization of *S. aureus*-containing phagolysosomes is without effect. The effect of making phagolysosomes harboring live GFP-expressing and eFluor-labeled *S. aureus* USA300 more alkaline was examined. In panel A, fluorescence-based proliferation assays were performed, and the representative images depict growth of intracellular *S. aureus* at 12 h postinfection. Macrophages after infection and gentamicin treatment (i.e., at 1.5 h postinfection) were left untreated or were treated with 1 μM ConA or 40 mM NH_4Cl, which were maintained on the cells throughout the experiment. These images are representative of at least three independent experiments. Scale bars equal ~10 μm. In panel B, the effect of ConA and NH_4Cl on the ability of macrophages to maintain acidified endosomes and lysosomes as revealed by LysoTracker Red DND-99 staining is shown. Images are of living cells stained with LysoTracker after pretreatment with either 1 μM ConA, 40 mM NH_4Cl, or no treatment at all and are representative of two independent experiments. Scale bars equal ~10 μm. In panel C, the bacterial burden of RAW macrophages in the presence or absence of ConA and NH_4Cl is shown. Data are the mean ± SEM fold change in CFU per milliliter at 6 h postinfection and are derived from four independent experiments. n.s. indicates not significant as determined by one-way ANOVA with a Dunnett's posttest *P* value of >0.05. In panel D, the effect of ConA and NH_4Cl on phagolysosomal replication of GFP-expressing *S. aureus* in primary human M-CSF-derived macrophages is shown. Fluorescence-based proliferation assays were performed as in panel A. The graph shows the fraction of macrophages that contained replicating bacteria in the presence or absence of ConA and NH_4Cl at 12 h postinfection. The data are the mean ± SEM derived from three

(Continued on next page)

throughout the infection. In these infections, the bacterial burden for wild-type *S. aureus* USA300(pALC2073) increased ~38-fold by 12 h postinfection, whereas pretreatment of macrophages with ConA surprisingly impaired wild-type growth (Fig. 4E). Consistent with our earlier observations (Fig. 3), we found that *graS*-deficient *S. aureus* did not proliferate within macrophages by 12 h postinfection, and pretreatment of macrophages with ConA failed to rescue bacterial growth (Fig. 4E). Importantly, complementation with *graS* in *trans* restored growth, as evidenced by the ~13-fold increase in bacterial burden in untreated macrophages. Interestingly, pretreatment of macrophages with ConA also impaired proliferation, as was observed for wild-type *S. aureus* (Fig. 4E). Taken together, these data indicate that exposure to acid in the phagolysosome engenders *S. aureus* with the ability to grow in this niche, and this requires the sensor kinase GraS. Consistent with this, we find that, when grown *in vitro* at pH 5.5 to mimic the measured pH of the phagolysosome, *graS*-deficient *S. aureus* cells grow similarly to wild-type bacteria, indicating that this level of acidity alone cannot account for the observed growth defect inside the SaCP (Fig. S4B). Finally, to determine whether the GraS sensor can perceive pH alone, we constructed a bioluminescent reporter to monitor the promoter activity of *mprF*, an established GraS-regulated gene. In wild-type *S. aureus* strain USA300, plasmid pGYLux::*mprF* made the bacteria bioluminescent, which was enhanced upon culture at pH 5.5 (Fig. 4F). In contrast, induction of bioluminescence at pH 5.5 was abrogated in *graS* bacteria carrying the same pGYLux::*mprF* plasmid (Fig. 4F), indicating *mprF* promoter activity is enhanced at acidic pH, via GraS.

GraS is required for acidic pH-dependent resistance of *S. aureus* to killing by polymyxin B and is required for resistance to LL-37 and reactive oxygen species. Previous work has shown that the GraXRS regulatory system is required for antimicrobial peptide (AP) resistance and that AP resistance can be modulated by acidic pH (26, 27). Presumably in the phagolysosome of the macrophage, these factors and others are experienced by *S. aureus* simultaneously and GraS plays an important role in enabling bacterial adaptation. Here, we explored the role GraS plays in mediating AP resistance at pH 5.5 to mimic the measured pH of the macrophage phagolysosome (Fig. 5A and B). To this end, the *S. aureus* USA300(pALC2073), *graS*(pALC2073), and *graS*(pGraS) strains were cultured in serum-free RPMI at pH 7.4 and 5.5 in the presence or absence of 64 μg/ml polymyxin B (PmB) or 12.5 μM human LL-37. All three strains, although able to grow in RPMI alone, failed to grow in RPMI in the presence of PmB (Fig. 5A). In contrast, at pH 5.5 and in the presence of PmB, only the wild-type *S. aureus* USA300(pALC2073) and *graS*(pGraS) strains grew well in the presence of PmB (Fig. 5A). Cultures of *S. aureus* in the presence of the human cathelicidin LL-37 at neutral and acidic pH did not demonstrate such dramatic differences in LL-37 resistance at pH 7.4 and 5.5 (Fig. 5B). Nevertheless, growth of the *graS*(pALC2073) strain was significantly reduced relative to that of wild-type and *graS*(pGraS) bacteria in the presence of LL-37 at pH 7.4 and 5.5, indicating GraS is required for LL-37 resistance under both conditions (Fig. 5B).

Within the phagolysosome, *S. aureus* would be expected to experience reactive oxygen species (ROS)-imposed stress, and previous work has indicated that GraXRS

FIG 4 Legend (Continued)
independent experiments using macrophages derived from three independent blood donors. n.s. denotes not significant with $P > 0.05$. The data presented in the graph have been normalized to the untreated condition for each experiment. In panel E, the bacterial burden of RAW macrophages infected with USA300 and the *graS* mutant carrying either the vector control or the GraS complementation vector is shown. Macrophages were also pretreated with 1 μM ConA prior to infection to inhibit V-ATPase function and lysosome acidification prior to the uptake of *S. aureus*. The data presented are the mean fold change in CFU per milliliter ± SEM at the indicated time relative to the bacterial burden obtained of each respective strain at 1.5 h postinfection (after gentamicin treatment) in the presence and absence of ConA. These data were derived from at least three experiments, and significance was determined by one-way ANOVA with Bonferroni's posttest. **, $P \leq 0.01$. In panel F, the graph shows the relative light production from wild-type *S. aureus* USA300 and the *graS* mutant each carrying plasmid pGYLux::*mprF*. The plotted data are the mean RLU ± SEM after 2 h of growth from a representative experiment in which each strain was analyzed in biological triplicate for each condition. These data were background subtracted, where background was taken as each strain transformed with empty pGYLux plasmid and cultured under the same conditions. Statistical significance was determined by one-way ANOVA with a Bonferroni's posttest. **, $P < 0.01$; ***, $P < 0.0001$.

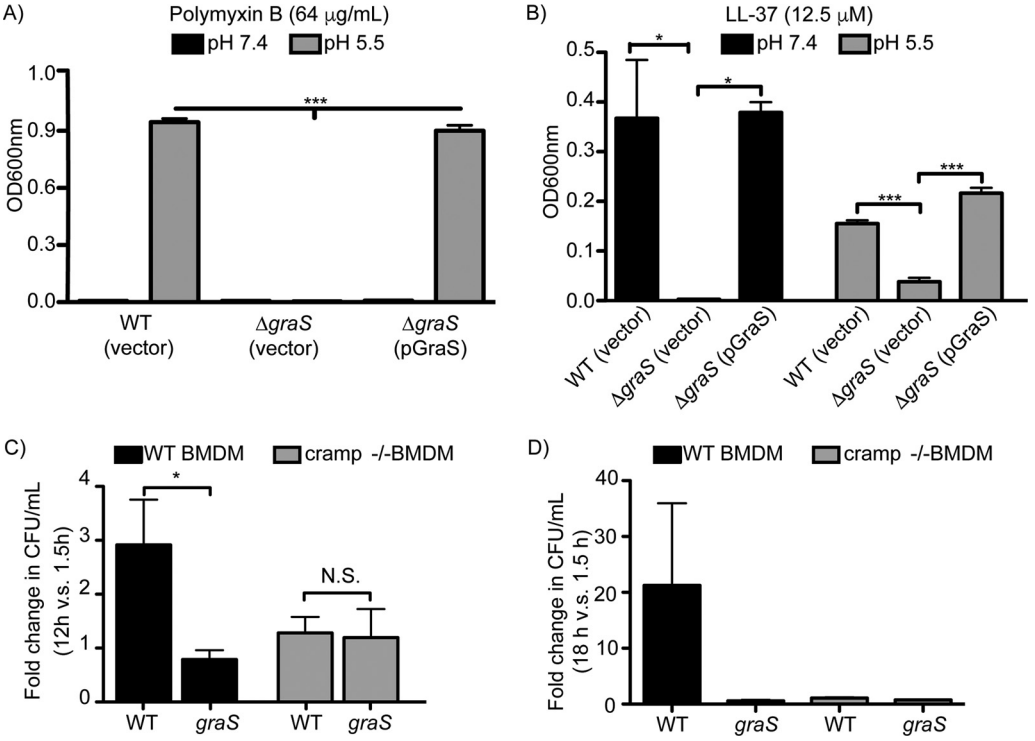

FIG 5 Acidic pH induces *S. aureus* resistance to select antimicrobial peptides, and peptide resistance requires *graS*. The resistance of *S. aureus* USA300 and a mutant strain lacking the *graS* gene to PmB (A) and LL-37 (B) in response to changes in pH is shown. In panel A, *S. aureus* USA300 carrying the vector control (pALC3073) and a *graS* mutant carrying either a vector control (pALC2073) or a GraS-encoding plasmid (pGraS) were cultured in RPMI 1640 at pH 7.4 or 5.5 in the presence 64 μg/ml polymyxin B (PmB). Shown is the endpoint OD_{600} after 24 h of growth under such culture conditions. The data are the mean OD_{600} $\pm$ SEM from three independent experiments with each strain cultured in biological triplicate for each. In panel B, similar experiments were performed, except the bacteria were cultured in the presence of 12.5 μM human LL-37 (B). In panels A and B, statistical significance was determined by Student's unpaired *t* test. *, $P \leq 0.05$; ***, $P \leq 0.001$. In panels C and D, the ability of *S. aureus* USA300 and *graS*-deficient bacteria to proliferate in wild-type and *cramp*$^{-/-}$ bone marrow-derived macrophages after infection at an MOI of 10 is shown. In panel C, the fold change in bacterial burden at 12 h versus 1.5 h postinfection is shown. These data are the mean $\pm$ SEM from three independent experiments with each strain analyzed in biological triplicate. *, $P < 0.05$ as determined by an unpaired Student's *t* test; N.S., not statistically significant. In panel D, the fold change in bacterial burden at 18 h postinfection, normalized to 1.5 h postinfection, is shown. These data are the mean $\pm$ SEM from a single experiment with each strain analyzed in 3 to 5 independent replicates.

contributes to ROS resistance (28). To determine whether ROS resistance in *S. aureus* is influenced by GraS and pH, the same strains were cultured in RPMI at pH 7.6 and 5.7 in the presence and absence of 10 μM paraquat (see Fig. S5 in the supplemental material). Remarkably, in the presence of paraquat at pH 7.6, all strains demonstrated very poor growth, but this growth impairment was alleviated at acidic pH (Fig. S5). Under these conditions, wild-type *S. aureus* USA300 grew on average ~32% better than the *graS* strain; however, in this instance, providing GraS in *trans* failed to complement the growth difference (Fig. S5). Taken together, these data indicate that GraS is required for *S. aureus* resistance to antimicrobial effectors found in phagolysosomes and bacterial killing can be affected by environmental pH.

GraS-deficient and wild-type *S. aureus* USA300 strains fail to proliferate in *cramp*$^{-/-}$ macrophages. Given that inactivation of *graS* results in sensitivity of *S. aureus* to antimicrobial peptides, we sought to determine whether infection of cathelicidin-deficient murine macrophages could rescue the growth defect of *graS* bacteria. To this end, macrophages were derived, using M-CSF, from the bone marrow of wild-type C57BL/6 and *cramp*$^{-/-}$ mice. The bone marrow-derived macrophages (BMDMs) were infected with either *S. aureus* USA300 or a *graS* mutant, and at 1.5 h postinfection, similar numbers of wild-type and mutant bacteria were recovered from macrophages of both backgrounds. By 12 h postinfection in C57BL/6 BMDMs, wild-type *S. aureus*

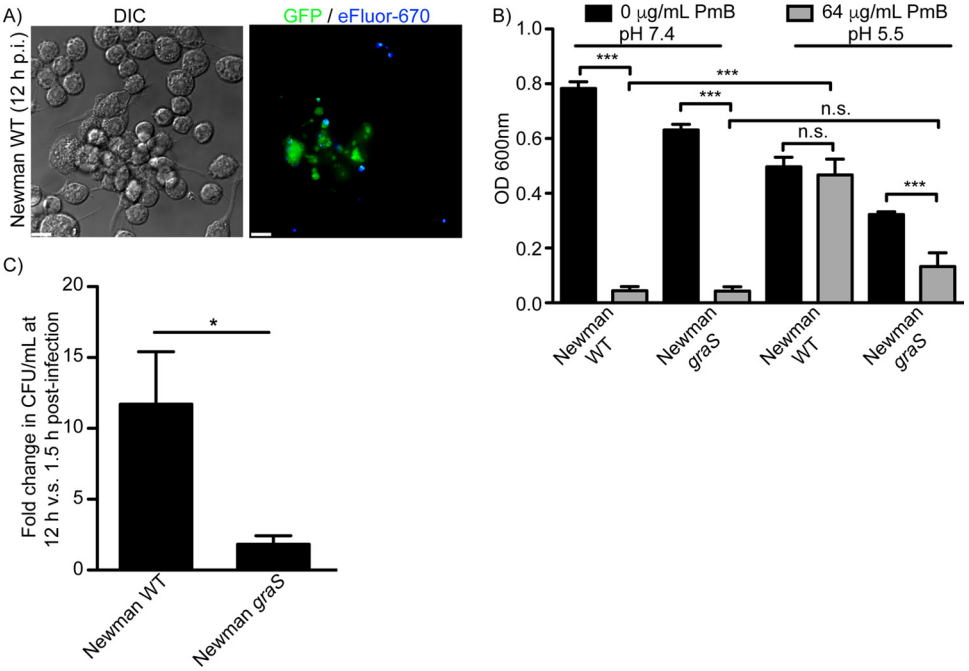

FIG 6 Growth of methicillin-sensitive *S. aureus* strain Newman in the presence of PmB and in macrophages requires *graS*. In panel A, the micrographs depict *S. aureus* strain Newman proliferating at 12 h postinfection in RAW macrophages. At this time, GFP-positive yet proliferation dye-negative bacteria represent *S. aureus* that had undergone intracellular replication. Scale bars equal 10 μm. In panel B, the ability of *S. aureus* strain Newman and a derivative lacking a functional *graS* gene to grow in the presence of PmB is shown. Wild-type and *graS* bacteria were cultured at pH 7.4 and 5.5 in the presence and absence of 64 μg/ml PmB, and the optical density (OD_{600}) was measured after 20 h of growth. The data are the mean OD_{600} reading $\pm$ SEM with each strain analyzed in biological triplicate in three independent experiments. ***, $P \leq 0.001$. In panel B, the inability of the *graS* mutant in the Newman background to grow inside macrophages is shown. Growth of the parental strain and the mutant expressed as a mean fold change $\pm$ SEM in CFU per milliliter at 12 h versus 1.5 h postinfection is shown. Statistical significance was determined by a Student's unpaired *t* test. *, $P \leq 0.05$.

USA300 had increased approximately 3-fold, whereas *graS* bacteria failed to proliferate (Fig. 5C). In *cramp*$^{-/-}$ M-CSF-derived macrophages, *graS* bacteria also failed to proliferate by 12 h postinfection; however, remarkably, USA300 also repeatedly failed to proliferate (Fig. 5C). Due to this striking observation, subsequent macrophage infections were carried out until 18 h postinfection to determine whether bacterial growth was simply delayed in *cramp*$^{-/-}$ macrophages (Fig. 5D). By 18 h postinfection, wild-type *S. aureus* USA300, in the presence of wild-type macrophages, grew to a high cell density due to the eventual escape from infected phagocytes and extracellular growth, as has been previously described (15) (Fig. 5D). In contrast, *graS* bacteria remain unable to proliferate even after 18 h in both wild-type and *cramp*$^{-/-}$ macrophages. In stark contrast, even at 18 h postinfection wild-type *S. aureus* USA300 failed to commence replicating in *cramp*$^{-/-}$ macrophages (Fig. 5D). These data suggest that *S. aureus* uses the presence of cathelicidin in the phagolysosome as a signal, through the Gra two-component regulatory system, to adapt to this hostile environment before proliferation proceeds.

Methicillin-sensitive *S. aureus* strain Newman requires GraS to grow within macrophages. Inactivation of GraS in *S. aureus* USA300 significantly impairs the ability of these bacteria to grow within the macrophage phagolysosome; however, we sought to confirm that this was not specific to the USA300 strain. We first demonstrated that the methicillin-sensitive *S. aureus* strain Newman can replicate inside RAW cells (Fig. 6A). Therefore, we transduced the *graS*::φNΣ mutation from the Nebraska transposon library into strain Newman. As a first step toward characterizing this strain, we sought to confirm that inactivation of *graS* renders Newman sensitive to antimicrobial peptide-dependent killing. To this end, we compared the growth of wild-type Newman

and its isogenic *graS* mutant in the presence and absence of 64 μg/ml PmB at pH 7.4 and 5.5 (Fig. 6B). Consistent with our USA300 data, we find that at neutral pH, neither wild-type nor mutant bacteria grow in the presence of 64 μg/ml PmB (Fig. 6B). In contrast at pH 5.5, strain Newman deficient for *graS* is highly sensitive to PmB and grows significantly less than the wild-type or the *graS* mutant in the absence of PmB. In contrast, wild-type Newman bacteria grow equally well in the presence and absence of PmB at pH 5.5, indicating that indeed in the methicillin-sensitive *S. aureus* background, *graS* is required for PmB resistance even at acidic pH (Fig. 6B). Next, we analyzed the ability of the Newman *graS* strain to replicate inside RAW macrophages. By 12 h postinfection, wild-type Newman achieves on average an ~10-fold increase in bacterial burden, which contrasts with the *graS* strain, which failed to replicate (Fig. 6C). Taken together, these data indicate that GraS is important for the intracellular replication of *S. aureus* and is not a unique requirement in strain USA300.

GraS-regulated *mprF* is required for *S. aureus* replication in macrophages. The multiple peptide resistance factor MprF catalyzes the formation of lysylphosphatidylglycerol (LPG) and contributes to antimicrobial peptide resistance in *S. aureus*. Moreover, as we have shown above, *mprF* promoter is activated in response to acidic pH through GraS (Fig. 4F). As such, we speculated that MprF might contribute to the survival of *S. aureus* within the phagolysosome. To analyze the importance of *mprF* for the replication of *S. aureus* in the macrophage, we utilized a mutant from the Nebraska transposon library carrying an inactivated copy of the *mprF* gene (*mprF*::φNΣ). As a first step toward characterizing the *mprF* mutant, growth of wild-type *S. aureus* USA300, USA300 *graS*, and USA300 *mprF* in the presence and absence of 64 μg/ml PmB at pH 7.4 and 5.5 was analyzed (Fig. 7A). As expected, at neutral pH each strain failed to grow in the presence of PmB yet grew equally well in the absence of the peptide (Fig. 7A). In contrast, at pH 5.5 wild-type *S. aureus* USA300 and the *mprF* mutant grew to similar optical densities in the presence of PmB, while the *graS* strain was dramatically impaired for growth (Fig. 7B). While these data indicated that the gene(s) downstream of GraS that contribute to PmB resistance must not be *mprF*, at least on its own, we considered that MprF might still play an important role for growth in the phagolysosome. To analyze this, we performed gentamicin protection assays using RAW macrophages in which the abilities of *S. aureus* USA300 and the *mprF* strain to grow over a 12-h infection were compared. In these experiments, wild-type *S. aureus* USA300 strain demonstrated an ~5-fold increase in bacterial density at 12 h compared to 1.5 h postinfection (Fig. 7C). In contrast, the *mprF* mutant when analyzed in parallel failed to yield an increased bacterial burden (Fig. 7C). These data indicate that *mprF* contributes to phagolysosomal growth of *S. aureus* but not to resistance to PmB at pH 5.5.

GraS and MprF are required for early stage survival of *S. aureus* within the murine liver. As our data show *graS* is required for the ability of *S. aureus* to proliferate within the macrophage phagolysosome *in vitro*. Therefore, we next investigated whether GraS would have a role in bacterial survival *in vivo* in the acute or early stages of a systemic infection. It has been demonstrated that during systemic infection, *S. aureus* is readily captured by Kupffer cells, the resident macrophages in the liver, and once captured reside in these cells for hours before they then begin to replicate (16). Since *S. aureus* remains confined to Kupffer cells at 8 h postinfection, we employed this model to determine whether GraS would contribute to bacterial survival in macrophages *in vivo*. To this end, BALB/c mice were injected via tail vein with ~5.0 $\times$ 10^6 cells of wild-type *S. aureus* USA300 or the *graS* or *mprF* mutant strain, and at 8 h postinfection, the bacterial burden for each strain in the murine liver was determined. At this time, each strain could be recovered from the liver, indicating none of the strains was completely eradicated. However, we found that significantly more wild-type *S. aureus* USA300 bacteria can be recovered from the liver 8 hpi compared to mice infected with the *graS* or *mprF* bacteria. These data indicate that GraS and the GraS-regulated MprF contribute to *S. aureus* survival in the liver, early in infection (i.e., 8 hpi), and presumably in Kupffer cells (Fig. 7D).

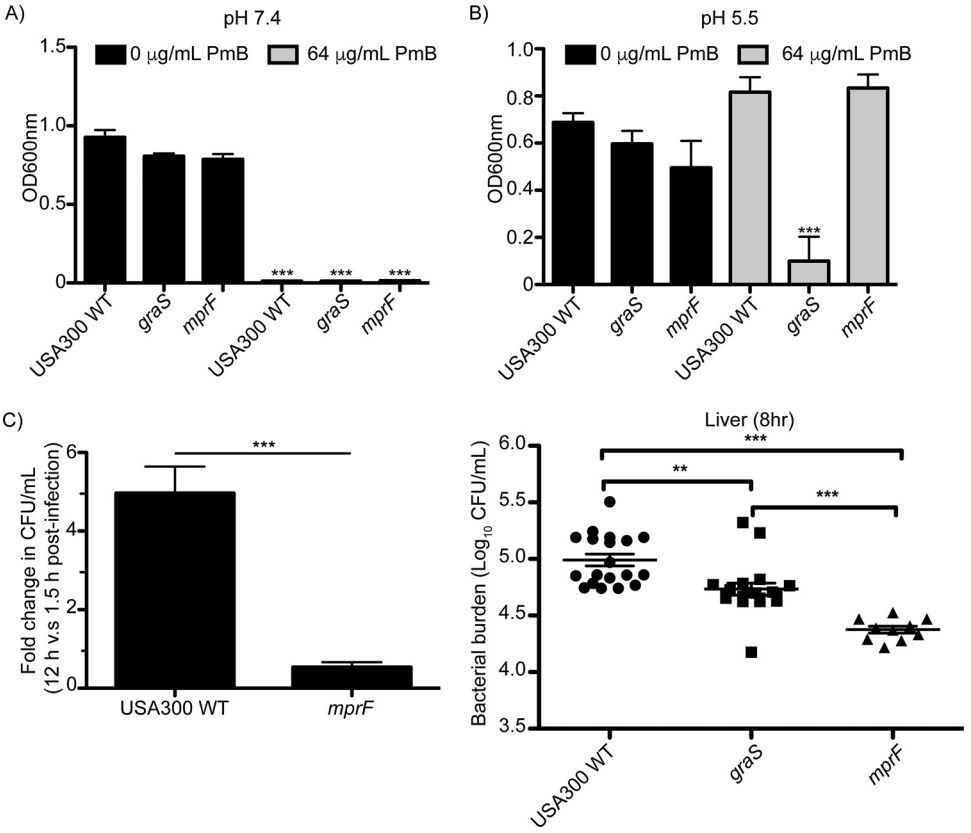

FIG 7 GraS and the downstream gene *mprF* are required for growth in macrophages and optimal survival in the murine liver in the early stages of systemic infection. The ability of *S. aureus* lacking the *mprF* gene to resist PmB-dependent growth restriction at pH 7.4 (A) and 5.5 (B) was determined. In panels A and B, bacteria were cultured in RPMI at the indicated pH in the presence and absence of 64 μg/ml PmB and growth was measured after 20 h at 37°C. Shown are the mean ± SEM optical density readings from two independent experiments with each strain cultured in biological triplicate in each experiment. In panel C, the ability of *mprF*-deficient *S. aureus* to grow inside RAW macrophages is shown. The data are the mean ± SEM from three independent experiments and are expressed as the fold change in CFU per milliliter at 12 h postinfection for wild-type *S. aureus* USA300 and the *mprF* mutant. The data were derived from at least three independent experiments, and statistical significance was determined by a Student's unpaired *t* test ($P \leq 0.0001$). The role of *graS* and *mprF* in the survival of *S. aureus* in the murine liver was determined at 8 h postinfection, when the bacteria are expected to reside within Kupffer cells. Mice infected with *S. aureus* via tail vein injection were sacrificed, and the bacterial burden in whole-liver homogenates was determined. The data are presented as the $\log_{10}$ CFU per milliliter, and each symbol represents the bacterial burden from one infected animal. The horizontal bars represent the mean ± SEM. Statistical significance was determined by a one-way ANOVA with Bonferroni's posttest to compare each mean. **, $P \leq 0.01$; ***, $P \leq 0.001$.

DISCUSSION

Staphylococcus aureus is a versatile pathogen seemingly capable of infecting and surviving in any niche of the body, illustrating the remarkable ability of this bacterium to circumvent immune mechanisms of the host. At the cellular level, the macrophage phagolysosome represents a highly microbicidal environment, and yet *S. aureus* proliferates within this niche (15, 16). How *S. aureus* evades killing and replicates inside phagolysosomes has not been determined, and here we demonstrate that *S. aureus* requires the sensor kinase GraS for phagolysosomal growth in murine and human macrophages. Moreover, we show that GraS contributes to *S. aureus* survival *in vivo* in the acute stages of systemic infection, coinciding with when the bacteria have been shown to reside in Kupffer cells (16). As an antimicrobial organelle, the phagolysosome is acidic, it can be enriched with toxic ROS, and it contains antimicrobial proteins and peptides (i.e., lysozyme and cathelicidin) that intoxicate ingested bacteria (reviewed in reference 29). In *S. aureus*, GraXRS regulates genes (e.g., *mprF*, *dltABCD*, and *vraFG*) (28, 30, 31) involved in antimicrobial peptide resistance, and our observation that bacteria

lacking GraS are unable to replicate within the macrophage phagolysosome further supports this notion. Here we have shown through fluorescence imaging that, in the context of the macrophage, *S. aureus* resides inside intact LAMP-1-positive phagolysosomes that are fully acidified, and this is where proliferation of phagocytosed *S. aureus* commences. Moreover, it is within these LAMP-1-positive phagolysosomes where *graS* cocci, despite being hemolytic (Fig. S1A), remain confined at least within the time frame (through 12 h postinfection) considered here.

Unlike other successful intracellular pathogens (e.g., *Listeria monocytogenes* and *Mycobacterium tuberculosis*) that disrupt phagosome maturation to evade phagolysosome fusion (reviewed in reference 11), we find that *S. aureus* resides inside mature phagolysosomes. Consequently, we find that acidic pH, a hallmark of phagolysosome fusion, acts as an environmental cue that elicits adaptation and increases the ability of *S. aureus* to replicate within this niche. We find that GraXRS is required for growth inside the macrophage phagolysosome, and through GraS, we find that *S. aureus* upregulates, in a pH-dependent manner, the expression of genes (e.g., *mprF*) that will promote survival in this antimicrobial compartment. Consistent with our observations, recent work has indicated that GraXRS is used by *S. aureus* to adapt and grow at acidic pH *in vitro*, independently demonstrating the GraS sensor allows *S. aureus* to perceive changes in environmental pH (32). The GraXRS system is known to play an important role in regulating antimicrobial peptide resistance in *S. aureus*, and our data further support this assertion. Here we find that acidic pH can modulate the intrinsic resistance of *S. aureus* to the antimicrobial compound PmB; however, the same effect is not apparent for LL-37, at least under the experimental conditions analyzed here, indicating the mechanisms of resistance for these two peptides are likely different. This is exemplified by inactivation of the GraS-regulated gene *mprF*, which has been shown to confer resistance to defensins (33), but does not render *S. aureus* sensitive to PmB even at acidic pH (Fig. 7B). Nevertheless, in the acidic milieu of the phagolysosome, *S. aureus* would upregulate Gra-regulated genes that through different mechanisms should allow the bacteria to better resist a broad-spectrum antimicrobial attack. Previous work has indicated that GraS in *S. aureus* is responsive to exposure to antimicrobial peptides as well (28, 31), and conceivably, APs and acidic pH are "sensed" by GraS. Detailed studies of the GraS sensor have revealed that its periplasmic loop and several critical residues contained therein are required for GraS signal transduction in response to antimicrobial peptide exposure (26, 34). It will be of interest to determine if the same residues in GraS are required for its pH-responsive functions as well as it may very well be a combination of these stimuli that leads to adaptation and growth of *S. aureus* in the macrophage phagolysosome. In agreement with this notion, we find that even in *cramp*$^{-/-}$ macrophages, wild-type *S. aureus* shows impaired growth compared to infection in wild-type macrophages. Conceivably, this is due to the absence of cathelicidin, which could operate as an environmental cue to which *S. aureus* adapts. Consistent with the importance of such cues for *S. aureus* growth, we also find that alkalinization of macrophage lysosomes, by pretreatment with an inhibitor of the V-ATPase, also impairs the intracellular growth of wild-type *S. aureus* USA300 in wild-type macrophages. This is in agreement with previous observations (18, 35), and the inability of *S. aureus* to grow in the absence of cathelicidin or phagosome acidification may not be unrelated. Indeed, cathelicidin is synthesized as a preprotein that must be proteolytically processed to become an active antimicrobial peptide (36). Given that lysosomal alkalinization impairs proteolytic activity (37), it is tempting to speculate that V-ATPase inhibition also abrogates cathelicidin processing. In this way, two stimuli that have now been shown to evoke GraS signaling would be eliminated. At the outset of these experiments, it was hypothesized that inhibition of phagosome acidification or the absence of cathelicidin would augment *S. aureus* growth, as has been observed for other bacterial pathogens (38, 39). However, from our experiments, it is clear that the interaction of *S. aureus* with the phagolysosomal environment is complex and additional antimicrobial effectors must also restrict *S. aureus* growth.

Previous work has suggested that *S. aureus* deploys toxins such as Hla or PSMα

peptides to mediate escape from the *S. aureus*-containing phagosome or to allow the bacteria to replicate within the macrophage (19, 20). The notion that *S. aureus* must escape the phagosome to replicate is incompatible with our molecular imaging data showing the subcellular niche in which phagocytosed *S. aureus* replicates is also acidic. Indeed, perforation of the limiting SaCP would lead to dissipation of any proton gradient and alkalinization of the vacuole. Moreover, the observation that *graS* bacteria, which are hemolytic, are unable to replicate within the macrophage challenges the notion that toxin production is required for *S. aureus* growth inside the macrophage. Many toxins (e.g., Hla, PSMα peptides, and LukAB) are either directly or indirectly regulated by Sae and Agr (21, 40), and considering the receptors (e.g., ADAM-10 and CD11b) required for cytotoxicity are displayed at the cell surface (41, 42), it is perhaps not unexpected that these systems are dispensable for growth inside the macrophage phagosome. It is important to emphasize that, in our study, we have focused on the ability of intracellular bacteria to grow inside the phagolysosome in the absence of an extracellular infection; in the latter case, it is well known that Agr- and Sae-regulated toxin production plays an important role in leukocyte intoxication (43–46). As mentioned above, Agr and Sae have been implicated in the ability of *S. aureus* to withstand the innate defenses of neutrophils and macrophages (18, 22, 24); however, our data reveal that these systems are dispensable for the replication of *S. aureus* in the macrophage phagolysosome. Presumably, the discrepancy between previous studies and the data we present here, at least in terms of the role that Agr plays in intracellular survival of *S. aureus*, is due to strain variation, use of distinct cells and or cell lines, and methodological differences, namely, the prolonged use of antibiotics. The notion that aminoglycoside antibiotics such as gentamicin, which are commonly used for *in vitro* infection assays, do not enter host cells is not accurate and is beginning to recede (15, 47–49). Nevertheless, several studies to date investigating macrophage infection by *S. aureus* have employed prolonged antibiotic treatment, which will have undoubtedly led, in some instances, to the characterization of intracellular antibiotic-treated bacteria. Regardless, the realization that *graS* is required for *S. aureus* proliferation within the macrophage phagolysosome and that acidic pH plays an important role in eliciting a GraS response represents an important step toward understanding, at the molecular level, how *S. aureus* can circumvent the innate immune function of macrophages in the intracellular environment.

MATERIALS AND METHODS

Reagents. The fluorescent cell proliferation dye eFluor-670 was from eBiosciences. Tetramethyl rhodamine isothiocyanate (TRITC)-conjugated wheat germ agglutinin (TMR-WGA), LysoTracker green DND-26, and FITC-dextran (molecular weight [MW], 10,000) were from Thermo Fisher Scientific. Concanamycin A (ConA) was purchased from Santa Cruz Biotechnology. Goat anti-human Alexa 488-, goat anti-human Cy3-, and goat anti-rat Cy3-conjugated antibodies were from Jackson ImmunoResearch, Inc. All restriction enzymes and T4 DNA ligase were from New England Biolabs, Inc. Polymyxin B, paraquat dichloride, and NH_4Cl were purchased from Sigma-Aldrich. LL-37 was purchased from AnaSpec, Inc.

Bacterial strains, bacterial plasmids, and culture conditions. *Escherichia coli* DH5α was used for cloning purposes and was cultured as previously described (50). All *S. aureus* strains and the plasmids used in this study are summarized in Table 1. Routine culture of all *S. aureus* was done as previously described (15) with antibiotics at the following concentrations as needed: erythromycin, 3 μg/ml; chloramphenicol, 12 μg/ml; lincomycin, 20 μg/ml; and tetracycline, 4 μg/ml.

For growth of *S. aureus* in tryptic soy broth (TSB) buffered at pH 7.4 and 5.5, TSB Tris-maleate buffer (0.1 M Tris and 0.1 M maleic acid) was used in place of water. pH stability of sterile medium was monitored prior to each experiment, and maintenance of pH in spent culture medium was monitored after each experiment. For growth curves at pH 7.4 and 5.5, bacterial proliferation was monitored using a BioScreen automated growth curve analyzer with 250-μl culture volumes and constant shaking at 37°C.

***S. aureus* mutant construction.** All gene deletions in *S. aureus* USA300 were performed using the procedures previously described (51). In some instances, phage 80α was used for transduction following standard procedures. Detailed methods used for the creation of each mutant strain are provided in Text S1 in the supplemental material.

Growth of *S. aureus* in the presence of polymyxin B, LL-37, or paraquat. Cells were cultured overnight in TSB at 37°C with shaking in the presence of antibiotics as necessary, pelleted, washed 1× with sterile saline, and then diluted to make a suspension with an optical density at 600 nm (OD_{600}) of 0.5. The cells were then diluted 1:100 into 1 ml bicarbonate-free RPMI 1640 set to pH 7.4 or 5.5 with and without antimicrobial peptide at the following final concentrations: PmB, 64 μg/ml; and LL-37, 12.5 μM.

Paraquat was used at a final concentration of 10 micro molar and in RPMI at pH 7.4 and 5.7. Optical density was evaluated after incubation with shaking at 37°C for 20 h, at which time an endpoint OD_{600} reading was measured.

Bioluminescence assay conditions. Overnight cultures of USA300(pGylux::*mprF*), USA300 *graS* (pGylux::*mprF*), and USA300 with empty vector pGylux were grown to stationary phase in TSB with chloramphenicol. Three biological replicate cultures were inoculated to an OD_{600} of 0.01 in either 25 ml of unbuffered TSB or TSB with 0.1 M MES (morpholineethanesulfonic acid) at pH 5.5 in a 125-ml Erlenmeyer flask and were grown at 37°C with 220 rpm. After 2 h, the number of relative light units (RLU) for each flask was measured 4 times, and the corrected RLU was calculated as the mean of these measurements minus the RLU for each strain carrying empty vector pGYlux cultured under identical conditions.

Mammalian tissue culture. RAW 264.7 macrophages and primary human M-CSF-derived macrophages were cultured as described previously (15). Blood was drawn from healthy volunteers in accordance with protocols approved by the University of Western Ontario Research Ethics Board. For all infections, macrophages were seeded into 12-well tissue culture dishes with 18-mm sterile glass coverslips as necessary.

Macrophage infection assays. All macrophage infections were performed as previously described (15). In brief, *S. aureus* cells grown overnight in TSB that were unopsonized were used to infect macrophages at a multiplicity of infection (MOI) of 10 unless otherwise indicated. Bacteria were washed once and diluted into serum-free RPMI 1640 medium (SF-RPMI). For the synchronization of infection, tissue culture plates were centrifuged for 2 min at 277 × *g* and then incubated for 30 min at 37°C in a humidified incubator with 5% CO_2. After 30 min, the medium was aspirated and replaced with SF-RPMI containing 100 μg/ml gentamicin for 1 h. After gentamicin treatment, infected cells were rinsed with 1 ml sterile 1× phosphate-buffered saline (PBS) and replaced with RPMI-containing serum. When necessary, infections were incubated with 1 μg/ml TMR-WGA for 2 min prior to 20 min of fixation in 4% (vol/vol) paraformaldehyde (PFA) at room temperature. Alternatively, infected macrophages were lysed in 0.5 ml PBS containing 0.1% (vol/vol) Triton X-100 and serially diluted for CFU determination. In some instances, ConA (1 μM) or NH_4Cl (40 mM) was used to treat macrophages prior to or after phagocytosis as appropriate. Once added, ConA and NH_4Cl were maintained throughout the duration of the experiment.

To enumerate gentamicin-protected bacteria and calculate the fold change in CFU per milliliter, macrophages were lysed in 0.5 ml 0.1% (vol/vol) Triton X-100 and serially diluted in sterile saline. The fold change in CFU per milliliter for each experiment was determined by dividing bacterial counts obtained at 6 or 12 h postinfection for a given strain by the count obtained for the same strain at 1.5 h postinfection (i.e., right after gentamicin treatment). This was done for every condition in every experiment.

Isolation of BMDMs. Wild-type C57BL/6 mice and B6.129X1-*Camp*^{tm1Rlg}/J male mice that were age matched were ordered from The Jackson Laboratory. At 6 to 8 weeks of age, bone marrow cells were extracted and cultured using standard procedures (52, 53). In brief, isolated bone marrow cells were plated at a density of 1×10^6 cells per 18-mm well of a 12-well tissue culture dish containing a sterile cover glass. Cells were differentiated and maintained in 1 ml of RPMI supplemented with 10% (vol/vol) non-heat-inactivated fetal bovine serum (FBS), 10 ng/ml recombinant murine M-CSF (PeproTech), and antibiotics. The medium was changed on days 3 and 5 postisolation; however, on day 5, cells were washed four times with sterile 1× PBS and maintained in the same medium but without antibiotic. Macrophages were utilized for phagocytosis assays on day 7 and were infected with *S. aureus* as described above.

Fluorescence proliferation assays. Proliferation assays were done as previously described (15), and macrophage infections were performed as described above. In some instances, dead bacteria were used for phagocytosis. To inactivate *S. aureus*, bacteria were first labeled with eFluor-670, fixed with 4% (vol/vol) PFA for 20 min at room temperature, and then incubated for 35 min at 57°C. Cells were then washed and diluted in SF-RPMI for infections as described above. The fluorescent spectra of GFP or mCherry are sufficiently different from that of eFluor-670, such that the emission of GFP and eFluor or mCherry and eFluor can easily be separated using conventional filter sets. Due to the fact that all of the bacteria at the start of an infection are positive for eFluor-670, of which there is a finite amount, the appearance of eFluor-negative bacteria within macrophages identifies bacterial populations that have replicated which appear negative due to dilution of the eFluor dye below detectable levels.

LAMP-1 immunostain. Detection of endogenous LAMP-1 in primary human M-CSF-derived macrophages and RAW 264.7 macrophages was done as previously described (15). Mouse anti-human LAMP-1 antibody (H4A3) and rat anti-mouse LAMP-1 antibody (1D4B) were both purchased as supernatants from the Developmental Studies Hybridoma Bank (DSHB), and the antibodies were deposited into the DSHB: H4A3 by J. T. August and J. E. K. Hildreth and 1D4B by J. T. August.

Dextran pulse-chase. RAW and primary human macrophages adhered to 18-mm glass coverslips were cultured overnight (~16 h) in RPMI 1640 with 5 or 10% FBS (vol/vol), respectively, and loaded with FITC-dextran (100 μg/ml) as previously described (29). Infections were performed as described above, and at 11 h postinfection, infected macrophages were analyzed by live-cell fluorescence imaging.

Assessment of phagosomal pH. For rapid detection of phagosomal acidification, live macrophages were stained for 10 min with 250 nM LysoTracker Red DND-99 or LysoTracker Green DND-26 as appropriate. Stained cells were washed with serum-free RPMI 1640 lacking the probe and imaged immediately by live-cell fluorescence microscopy. When necessary, cells were pretreated with 1 μM ConA or 40 mM NH_4Cl for 1 h prior to LysoTracker staining.

Ratiometric measurements of phagosomal pH were done using FITC-dextran according the work of Ohkuma and Poole (25) and following the protocol described by Canton and Grinstein (54). Additional details are provided in Text S1.

Fluorescence microscopy. Wide-field fluorescence microscopy was performed on a Leica DMI6000 B inverted microscope equipped with 40× (NA 1.3), 63× (NA 1.4), and 100× (NA 1.4) oil immersion PL-Apo objectives, a Leica 100-W Hg high-pressure light source, and a Photometrics Evolve 512 Delta EM-CCD camera. This microscope is also outfitted with an objective warmer and an enclosed heated stage insert with CO_2 perfusion (Live Cell Instruments). This microscope is equipped with the ET-Sedat-quad 89000 series excitation and emission filter set (Chroma Technologies) for DAPI (4′,6-diamidino-2-phenylindole), GFP/FITC, Cy3/Alexa 555, and Cy5/Alexa 647 imaging. For live-cell imaging, coverslips carrying macrophages were placed in a magnetic imaging chamber and bathed in SF-RPMI buffered with Na bicarbonate and 25 mM HEPES. Live-cell imaging employed a heated stage and objective warmer set to 37°C and in the presence of 5% CO_2 as necessary.

Images were acquired as z-series, and when appropriate, the raw data were deconvolved using the Leica LAS X software. This was done for LAMP-1 images, and the micrographs depicted represent the sum of the fluorescence from consecutive deconvolved z-slices. Images were contrast cropped, contrast enhanced linearly, and merged in ImageJ. The gamma was never altered, and fluorescence intensity measurements were only made on raw data.

Murine systemic infection model. Bacteria were cultured as previously described (50). Bacterial suspensions were diluted to an OD_{600} equal to ~0.3 (5.0×10^7 CFU/ml) and used for injection. Six-week-old female BALB/c mice (Charles River Laboratories, Inc.) were injected via tail vein with 100 μl of bacterial suspension, and at 8 h postinfection, mice were anesthetized and then euthanized, and livers were harvested for plating. Extracted organs were placed into 3 ml of ice-cold 0.1% (vol/vol) Triton X-100 in 1× PBS and homogenized for 5 min by ballistic disruption in a Bullet Blender Storm (Next Advance, Troy, NY). Homogenates were serially diluted 10-fold and plated onto tryptic soy agar (TSA) for enumeration of the bacterial burden.

Ethics statement. Blood was obtained, with written permission, only from healthy adult volunteers, in compliance with protocol 109059 approved by the Office of Research Ethics at the University of Western Ontario. All animal protocols (protocol 2017-028) were reviewed and approved by the University of Western Ontario Animal Use Subcommittee, a subcommittee of the University Council on Animal Care. Protocols adhered to guidelines set out by the Canadian Council on Animal Care.

Statistical analyses and software. All statistical analyses were performed using GraphPad Prism software (San Diego, CA). When appropriate, one-way analysis of variance (ANOVA) and unpaired *t* tests were performed to determine statistical significance, with a *P* value cutoff of ≤ 0.05 to establish significance. Where appropriate, Bonferroni's and Dunnett's *post hoc* tests were performed to directly compare experimental means.

SUPPLEMENTAL MATERIAL

Supplemental material for this article may be found at https://doi.org/10.1128/mBio.01143-18.

TEXT S1, DOCX file, 0.1 MB.

FIG S1, TIF file, 4.5 MB.

FIG S2, TIF file, 4.5 MB.

FIG S3, TIF file, 1 MB.

FIG S4, TIF file, 0.3 MB.

FIG S5, TIF file, 0.3 MB.

ACKNOWLEDGMENTS

We thank Patrick Rudak at the University of Western Ontario for assistance in producing bone marrow-derived macrophages.

This research was funded by operating grants from the Canadian Institutes of Health Research to D.E.H. and from Cystic Fibrosis Canada to R.S.F. and D.E.H. Work in the laboratory of M.J.M. is funded by a discovery grant from the Natural Sciences and Engineering Research Council of Canada. The funders had no role in study design, data collection and analysis, decision to publish, or preparation of the manuscript.

REFERENCES

1. Montgomery CP, Boyle-Vavra S, Adem PV, Lee JC, Husain AN, Clasen J, Daum RS. 2008. Comparison of virulence in community-associated methicillin-resistant *Staphylococcus aureus* pulsotypes USA300 and USA400 in a rat model of pneumonia. J Infect Dis 198:561–570. https://doi.org/10.1086/590157.
2. Moore CL, Hingwe A, Donabedian SM, Perri MB, Davis SL, Haque NZ, Reyes K, Vager D, Zervos MJ. 2009. Comparative evaluation of epidemiology and outcomes of methicillin-resistant *Staphylococcus aureus* (MRSA) USA300 infections causing community- and healthcare-associated infections. Int J Antimicrob Agents 34:148–155. https://doi.org/10.1016/j.ijantimicag.2009.03.004.
3. Kennedy AD, Otto M, Braughton KR, Whitney AR, Chen L, Mathema B, Mediavilla JR, Byrne KA, Parkins LD, Tenover FC, Kreiswirth BN, Musser JM, DeLeo FR. 2008. Epidemic community-associated methicillin-

resistant *Staphylococcus aureus*: recent clonal expansion and diversification. Proc Natl Acad Sci U S A 105:1327–1332. https://doi.org/10.1073/pnas.0710217105.
4. Cieslak TJ, Ottolini MG, O'Neill KM, Lampe RM. 1993. *Staphylococcus aureus* meningitis associated with pyogenic infection of the sacroiliac joint. South Med J 86:1175–1178. https://doi.org/10.1097/00007611-199310000-00023.
5. Daum RS. 2007. Clinical practice. Skin and soft tissue infections caused by methicillin-resistant *Staphylococcus aureus*. N Engl J Med 357:380–390. https://doi.org/10.1056/NEJMcp070747.
6. Gonzalez BE, Martinez-Aguilar G, Hulten KG, Hammerman WA, Coss-Bu J, Avalos-Mishaan A, Mason EOJ, Kaplan SL. 2005. Severe staphylococcal sepsis in adolescents in the era of community-acquired methicillin-resistant *Staphylococcus aureus*. Pediatrics 115:642–648. https://doi.org/10.1542/peds.2004-2300.
7. Boucher H, Miller LG, Razonable RR. 2010. Serious infections caused by methicillin-resistant *Staphylococcus aureus*. Clin Infect Dis 51(Suppl 2):S183–S197. https://doi.org/10.1086/653519.
8. Spaan AN, Van Strijp JAG, Torres VJ. 2017. Leukocidins: staphylococcal bi-component pore-forming toxins find their receptors. Nat Rev Microbiol 15:435–447. https://doi.org/10.1038/nrmicro.2017.27.
9. Alonzo F, III, Torres VJ. 2014. The bicomponent pore-forming leucocidins of *Staphylococcus aureus*. Microbiol Mol Biol Rev 78:199–230. https://doi.org/10.1128/MMBR.00055-13.
10. Flannagan RS, Jaumouillé V, Grinstein S. 2012. The cell biology of phagocytosis. Annu Rev Pathol 7:61–98. https://doi.org/10.1146/annurev-pathol-011811-132445.
11. Flannagan RS, Cosío G, Grinstein S. 2009. Antimicrobial mechanisms of phagocytes and bacterial evasion strategies. Nat Rev Microbiol 7:355–366. https://doi.org/10.1038/nrmicro2128.
12. Lukacs GL, Rotstein OD, Grinstein S. 1990. Phagosomal acidification is mediated by a vacuolar-type H^+-ATPase in murine macrophages. J Biol Chem 265:21099–21107.
13. Lukacs GL, Rotstein OD, Grinstein S. 1991. Determinants of the phagosomal pH in macrophages. In situ assessment of vacuolar H^+-ATPase activity, counterion conductance, and H^+ "leak." J Biol Chem 266:24540–24548.
14. Lehar SM, Pillow T, Xu M, Staben L, Kajihara KK, Vandlen R, DePalatis L, Raab H, Hazenbos WL, Morisaki JH, Kim J, Park S, Darwish M, Lee BC, Hernandez H, Loyet KM, Lupardus P, Fong R, Yan D, Chalouni C, Luis E, Khalfin Y, Plise E, Cheong J, Lyssikatos JP, Strandh M, Koefoed K, Andersen PS, Flygare JA, Wah Tan M, Brown EJ, Mariathasan S. 2015. Novel antibody-antibiotic conjugate eliminates intracellular *S. aureus*. Nature 527:323–328. https://doi.org/10.1038/nature16057.
15. Flannagan RS, Heit B, Heinrichs DE. 2016. Intracellular replication of *Staphylococcus aureus* in mature phagolysosomes in macrophages precedes host cell death, and bacterial escape and dissemination. Cell Microbiol 18:514–535. https://doi.org/10.1111/cmi.12527.
16. Surewaard BGJ, Deniset JF, Zemp FJ, Amrein M, Otto M, Conly J, Omri A, Yates RM, Kubes P. 2016. Identification and treatment of the *Staphylococcus aureus* reservoir in vivo. J Exp Med 213:1141–1151. https://doi.org/10.1084/jem.20160334.
17. Gresham HD, Lowrance JH, Caver TE, Wilson BS, Cheung AL, Lindberg FP. 2000. Survival of *Staphylococcus aureus* inside neutrophils contributes to infection. J Immunol 164:3713–3722. https://doi.org/10.4049/jimmunol.164.7.3713.
18. Tranchemontagne ZR, Camire RB, O'Donnell VJ, Baugh J, Burkholder KM. 2016. *Staphylococcus aureus* strain USA300 perturbs acquisition of lysosomal enzymes and requires phagosomal acidification for survival inside macrophages. Infect Immun 84:241–253. https://doi.org/10.1128/IAI.00704-15.
19. Kubica M, Guzik K, Koziel J, Zarebski M, Richter W, Gajkowska B, Golda A, Maciag-Gudowska A, Brix K, Shaw L, Foster T, Potempa J. 2008. A potential new pathway for *Staphylococcus aureus* dissemination: the silent survival of *S. aureus* phagocytosed by human monocyte-derived macrophages. PLoS One 3:e1409. https://doi.org/10.1371/journal.pone.0001409.
20. Grosz M, Kolter J, Paprotka K, Winkler A-C, Schäfer D, Chatterjee SS, Geiger T, Wolz C, Ohlsen K, Otto M, Rudel T, Sinha B, Fraunholz M. 2014. Cytoplasmic replication of *Staphylococcus aureus* upon phagosomal escape triggered by phenol-soluble modulin α. Cell Microbiol 16:451–465. https://doi.org/10.1111/cmi.12233.
21. Dunman PM, Murphy E, Haney S, Palacios D, Tucker-Kellogg G, Wu S, Brown EL, Zagursky RJ, Shlaes D, Projan SJ. 2001. Transcription profiling-based identification of *Staphylococcus aureus* genes regulated by the *agr* and/or *sarA* loci. J Bacteriol 183:7341–7353. https://doi.org/10.1128/JB.183.24.7341-7353.2001.
22. Voyich JM, Vuong C, DeWald M, Nygaard TK, Kocianova S, Griffith S, Jones J, Iverson C, Sturdevant DE, Braughton KR, Whitney AR, Otto M, DeLeo FR. 2009. The SaeR/S gene regulatory system is essential for innate immune evasion by *Staphylococcus aureus*. J Infect Dis 199:1698–1706. https://doi.org/10.1086/598967.
23. Schmitt J, Joost I, Skaar EP, Herrmann M, Bischoff M. 2012. Haemin represses the haemolytic activity of *Staphylococcus aureus* in an Sae-dependent manner. Microbiology 158:2619–2631. https://doi.org/10.1099/mic.0.060129-0.
24. Pang YY, Schwartz J, Thoendel M, Ackermann LW, Horswill AR, Nauseef WM. 2010. Agr-dependent interactions of *Staphylococcus aureus* USA300 with human polymorphonuclear neutrophils. J Innate Immun 2:546–559. https://doi.org/10.1159/000319855.
25. Ohkuma S, Poole B. 1978. Fluorescence probe measurement of the intralysosomal pH in living cells and the perturbation of pH by various agents. Proc Natl Acad Sci U S A 75:3327–3331. https://doi.org/10.1073/pnas.75.7.3327.
26. Chaili S, Cheung AL, Bayer AS, Xiong YQ, Waring AJ, Memmi G, Donegan N, Yang SJ, Yeaman MR. 2016. The GraS sensor in *Staphylococcus aureus* mediates resistance to host defense peptides differing in mechanisms of action. Infect Immun 84:459–466. https://doi.org/10.1128/IAI.01030-15.
27. Walkenhorst WF, Klein JW, Vo P, Wimley WC. 2013. pH dependence of microbe sterilization by cationic antimicrobial peptides. Antimicrob Agents Chemother 57:3312–3320. https://doi.org/10.1128/AAC.00063-13.
28. Falord M, Mäder U, Hiron A, Débarbouillé M, Msadek T. 2011. Investigation of the *Staphylococcus aureus* GraSR regulon reveals novel links to virulence, stress response and cell wall signal transduction pathways. PLoS One 6:e21323. https://doi.org/10.1371/journal.pone.0021323.
29. Flannagan RS, Heit B, Heinrichs DE. 2015. Antimicrobial mechanisms of macrophages and the immune evasion strategies of *Staphylococcus aureus*. Pathogens 4:826–868. https://doi.org/10.3390/pathogens4040826.
30. Falord M, Karimova G, Hiron A, Msadek T. 2012. GraXSR proteins interact with the VraFG ABC transporter to form a five-component system required for cationic antimicrobial peptide sensing and resistance in *Staphylococcus aureus*. Antimicrob Agents Chemother 56:1047–1058. https://doi.org/10.1128/AAC.05054-11.
31. Li M, Cha DJ, Lai Y, Villaruz AE, Sturdevant DE, Otto M. 2007. The antimicrobial peptide-sensing system aps of *Staphylococcus aureus*. Mol Microbiol 66:1136–1147. https://doi.org/10.1111/j.1365-2958.2007.05986.x.
32. Villanueva M, García B, Valle J, Rapún B, Ruiz de los Mozos I, Solano C, Martí M, Penadés JR, Toledo-Arana A, Lasa I. 2018. Sensory deprivation in *Staphylococcus aureus*. Nat Commun 9:523. https://doi.org/10.1038/s41467-018-02949-y.
33. Peschel A, Jack RW, Otto M, Collins LV, Staubitz P, Nicholson G, Kalbacher H, Nieuwenhuizen WF, Jung G, Tarkowski A, van Kessel KP, van Strijp JA. 2001. *Staphylococcus aureus* resistance to human defensins and evasion of neutrophil killing via the novel virulence factor MprF is based on modification of membrane lipids with L-lysine. J Exp Med 193:1067–1076. https://doi.org/10.1084/jem.193.9.1067.
34. Cheung AL, Bayer AS, Yeaman MR, Xiong YQ, Waring AJ, Memmi G, Donegan N, Chaili S, Yang SJ. 2014. Site-specific mutation of the sensor kinase GraS in *Staphylococcus aureus* alters the adaptive response to distinct cationic antimicrobial peptides. Infect Immun 82:5336–5345. https://doi.org/10.1128/IAI.02480-14.
35. Sedlyarov V, Eichner R, Girardi E, Essletzbichler P, Goldmann U, Nunes-Hasler P, Srndic I, Moskovskich A, Heinz LX, Kartnig F, Bigenzahn JW, Rebsamen M, Kovarik P, Demaurex N, Superti-Furga G. 2018. The bicarbonate transporter SLC4A7 plays a key role in macrophage phagosome acidification. Cell Host Microbe 23:766–774.e5.
36. Pestonjamasp VK, Huttner KH, Gallo RL. 2001. Processing site and gene structure for the murine antimicrobial peptide CRAMP. Peptides 22:1643–1650. https://doi.org/10.1016/S0196-9781(01)00499-5.
37. Coen K, Flannagan RS, Baron S, Carraro-Lacroix LR, Wang D, Vermeire W, Michiels C, Munck S, Baert V, Sugita S, Wuytack F, Hiesinger PR, Grinstein S, Annaert W. 2012. Lysosomal calcium homeostasis defects, not proton pump defects, cause endo-lysosomal dysfunction in PSEN-deficient cells. J Cell Biol 198:23–35. https://doi.org/10.1083/jcb.201201076.
38. Sonawane A, Santos JC, Mishra BB, Jena P, Progida C, Sorensen OE, Gallo R, Appelberg R, Griffiths G. 2011. Cathelicidin is involved in the intracel-

lular killing of mycobacteria in macrophages. Cell Microbiol 13:1601–1617. https://doi.org/10.1111/j.1462-5822.2011.01644.x.
39. Rosenberger CM, Gallo RL, Finlay BB. 2004. Interplay between antibacterial effectors: a macrophage antimicrobial peptide impairs intracellular Salmonella replication. Proc Natl Acad Sci U S A 101:2422–2427. https://doi.org/10.1073/pnas.0304455101.
40. Bronner S, Monteil H, Prévost G. 2004. Regulation of virulence determinants in *Staphylococcus aureus*: complexity and applications. FEMS Microbiol Rev 28:183–200. https://doi.org/10.1016/j.femsre.2003.09.003.
41. Wilke GA, Bubeck Wardenburg J. 2010. Role of a disintegrin and metalloprotease 10 in *Staphylococcus aureus* alpha-hemolysin-mediated cellular injury. Proc Natl Acad Sci U S A 107:13473–13478. https://doi.org/10.1073/pnas.1001815107.
42. DuMont AL, Yoong P, Day CJ, Alonzo F, III, McDonald WH, Jennings MP, Torres VJ. 2013. *Staphylococcus aureus* LukAB cytotoxin kills human neutrophils by targeting the CD11b subunit of the integrin Mac-1. Proc Natl Acad Sci U S A 110:10794–10799. https://doi.org/10.1073/pnas.1305121110.
43. Scherr TD, Hanke ML, Huang O, James DB, Horswill AR, Bayles KW, Fey PD, Torres VJ, Kielian T. 2015. *Staphylococcus aureus* biofilms induce macrophage dysfunction through leukocidin AB and alpha-toxin. mBio 6:e01021-15. https://doi.org/10.1128/mBio.01021-15.
44. Kitur K, Parker D, Nieto P, Ahn DS, Cohen TS, Chung S, Wachtel S, Bueno S, Prince A. 2015. Toxin-induced necroptosis is a major mechanism of *Staphylococcus aureus* lung damage. PLoS Pathog 11:e1004820. https://doi.org/10.1371/journal.ppat.1004820.
45. Montgomery CP, Boyle-Vavra S, Daum RS. 2010. Importance of the global regulators Agr and SaeRS in the pathogenesis of CA-MRSA USA300 infection. PLoS One 5:e15177. https://doi.org/10.1371/journal.pone.0015177.
46. Zurek OW, Nygaard TK, Watkins RL, Pallister KB, Torres VJ, Horswill AR, Voyich JM. 2014. The role of innate immunity in promoting SaeR/S-mediated virulence in *Staphylococcus aureus*. J Innate Immun 6:21–30. https://doi.org/10.1159/000351200.
47. VanCleave TT, Pulsifer AR, Connor MG, Warawa JM, Lawrenz MB. 2017. Impact of gentamicin concentration and exposure time on intracellular *Yersinia pestis*. Front Cell Infect Microbiol 7:505. https://doi.org/10.3389/fcimb.2017.00505.
48. Drevets DA, Canono BP, Leenen PJM, Campbell PA. 1994. Gentamicin kills intracellular *Listeria monocytogenes*. Infect Immun 62:2222–2228.
49. Menashe O, Kaganskaya E, Baasov T, Yaron S. 2008. Aminoglycosides affect intracellular *Salmonella enterica* serovars Typhimurium and Virchow. Antimicrob Agents Chemother 52:920–926. https://doi.org/10.1128/AAC.00382-07.
50. Sheldon JR, Marolda CL, Heinrichs DE. 2014. TCA cycle activity in *Staphylococcus aureus* is essential for iron-regulated synthesis of staphyloferrin A, but not staphyloferrin B: the benefit of a second citrate synthase. Mol Microbiol 92:824–839. https://doi.org/10.1111/mmi.12593.
51. Bae T, Schneewind O. 2006. Allelic replacement in *Staphylococcus aureus* with inducible counter-selection. Plasmid 55:58–63. https://doi.org/10.1016/j.plasmid.2005.05.005.
52. Davis BK. 2013. Isolation, culture, and functional evaluation of bone marrow-derived macrophages. Methods Mol Biol 1031:27–35. https://doi.org/10.1007/978-1-62703-481-4_3.
53. Weischenfeldt J, Porse B. 2008. Bone marrow-derived macrophages (BMM): isolation and applications. Cold Spring Harb Protoc 2008:pdb.prot5080. https://doi.org/10.1101/pdb.prot5080.
54. Canton J, Grinstein S. 2017. Measuring phagosomal pH by fluorescence microscopy. Methods Mol Biol 1519:185–199. https://doi.org/10.1007/978-1-4939-6581-6_12.
55. Duthie ES, Lorenz LL. 1952. Staphylococcal coagulase; mode of action and antigenicity. J Gen Microbiol 6:95–107. https://doi.org/10.1099/00221287-6-1-2-95.
56. Kreiswirth BN, Löfdahl S, Betley MJ, O'Reilly M, Schlievert PM, Bergdoll MS, Novick RP. 1983. The toxic shock syndrome exotoxin structural gene is not detectably transmitted by a prophage. Nature 305:709–712. https://doi.org/10.1038/305709a0.
57. Boles BR, Horswill AR. 2008. Agr-mediated dispersal of *Staphylococcus aureus* biofilms. PLoS Pathog 4:e1000052. https://doi.org/10.1371/journal.ppat.1000052.
58. Sayedyahossein S, Xu SX, Rudkouskaya A, McGavin MJ, McCormick JK, Dagnino L. 2015. *Staphylococcus aureus* keratinocyte invasion is mediated by integrin-linked kinase and Rac1. FASEB J 29:711–723. https://doi.org/10.1096/fj.14-262774.
59. Gries CM, Sadykov MR, Bulock LL, Chaudhari SS, Thomas VC, Bose JL, Bayles KW. 2016. Potassium uptake modulates *Staphylococcus aureus* metabolism. mSphere 1:e00125-16. https://doi.org/10.1128/mSphere.00125-16.
60. Bateman BT, Donegan NP, Jarry TM, Palma M, Cheung AL. 2001. Evaluation of a tetracycline-inducible promoter in *Staphylococcus aureus* in vitro and in vivo and its application in demonstrating the role of *sigB* in microcolony formation. Infect Immun 69:7851–7857. https://doi.org/10.1128/IAI.69.12.7851-7857.2001.
61. Mesak LR, Yim G, Davies J. 2009. Improved lux reporters for use in *Staphylococcus aureus*. Plasmid 61:182–187. https://doi.org/10.1016/j.plasmid.2009.01.003.